

Subject: **Revision of HESS-2019-430**

Dear Editors,

Thank you for your letter and for the reviewers' comments concerning our manuscript entitled "**A Universal Multifractal Approach to Assessment of Spatiotemporal Extreme Precipitation over the Loess Plateau of China**".

We quite appreciate your favorite consideration and the reviewer's insightful comments. These comments are all valuable and very helpful for revising and improving our paper, as well as the important guiding significance to our researches. We have studied all the comments from the three anonymous reviewers and the short comments from Zhihua Shi carefully and have made corrections which we hope to meet with approval. The point-to-point responses to all the comments are as follows.

### **Comments from Editor**

Please, address all referees' comment according to your reply, with special care for the method description which was the object of the more fundamental comments. Apart from the discussion about the method description and validity, the manuscript was appreciated and possibly it will be suitable for publication in HESS after revision.

Reply: Thank you very much for your favorite consideration. Both indices and methodology description were revised according to comments from all reviewers.

### **Comments from Anonymous Referee #1**

In the manuscript "A Universal Multifractal Approach to Assessment of Spatiotemporal Extreme Precipitation over the Loess Plateau of China". The authors try to proposal approach to identify the extreme precipitation events (EP), which is vital to the formation of soil erosion, and thereby to assess the spatiotemporal characteristics of the EP in the Loess Plateau (LP) during long term of 1961-2015. The study is interesting because providing new understanding about the spatiotemporal characteristics of EP in the LP. Meanwhile, the results are useful and contribute to the risk management (such as the soil erosion) in the LP. In my view, the MS may be suitable to be published in Hydrology and Earth System Sciences after minor revision.

Reply: Thank you very much for your favorite consideration and detailed suggestions. We have studied all the comments carefully and have made corrections.

**General comments**

The paper is well written and the results are well presented. Bibliography very exhaustive. The analyzed dataset is interesting and the results can be useful to improve the knowledge of spatiotemporal characteristics of EP and could be potentially useful for risk management. The results show that the approach integrating the universal multifractal approach and segmentation algorithm based on parametric statistical method can be used to identify the EP events. Then, giving a detailed description about the spatiotemporal characteristics of EP. What's more, the rationality of EP results is explained and verified through the relationship between EP with the spatial characteristics of soil erosion. Therefore, the presented results are robust and add new knowledge on those relevant eco-hydrologic study and management.

Reply: We quite appreciate your favorite consideration and insightful comments.

### Major comments:

1. Please explain the calculation of each indices of extreme precipitation in detail. It can help the readers to understand the meaning of the indices. Such as how to calculate the MEP?

Reply: More detailed information about the calculation of each indices were introduced in the revision of the manuscript.

See Lines 180-188, 201-204.

2. L319-326: Please strengthen this paragraph. How do you get the condition about the recovery of vegetation from the EP intensity?

Reply: Thanks for your suggestion. In this paragraph, we tried to discuss the intra-annual distribution of EP causing natural hazards in the LP. The day with highest EPF happens earlier than wettest day, indicating the climate reason why there is serious erosion in the LP. The paragraph was strengthened.

See Lines 360-367.

### Specific comments

1. There is a lack of the specific meaning of EPT (threshold of extreme precipitation), please briefly explain it in the "Introduction".

Reply: Thanks. The specific meaning of EPT was introduced.

See Lines 65-67.

2. Please include all the indices used in your study in Table 1. Such as EPS.

Reply: Sorry for my carelessness. All indices were introduced.

See Lines 180-205.

3. What is the difference of EPS and EPSI?

Reply: Sorry for my carelessness, EPS is EP severity, and "EPSI" was deleted, as shown in Table 1.

4. L 19: Please replace “scare” with “scarce”.

Reply: Thanks for your reminding. The word was corrected.

See Line 20.

5. L148: What is the specific criterion of “approximately equal” in the selection of EPT?

Reply: As shown in Figure 1, firstly, these abrupt points are the alternative EPT, and then the point and its corresponding variance with gentle slope on the right but deep slope on the left was determined as EPT in a station. The sentence was rephrased.

See Lines 175-177.

6. L159: Please explain the specific meaning of “ $n$ ” in the equation.

Reply: The parameter  $n$  was defined.

See Line 183.

7. L165: Is the PF represents EPF? Please illustrate the equation in detail

Reply: Yes.  $P_F$  was used to present EPF in the manuscript. The parameter was replaced by its abbreviation, EPF, in the Revision.

See Lines 183-186.

8. L195: Why the missing data were replaced by a value of 0 in your paper?

Reply: Thanks for your detailed question. The very few missing data were replaced by zeros because precipitation days account for <20% in the Loess Plateau.

9. L208: Please delete “from” after “50 mm/d”.

Reply: Thanks. It was corrected.

See Line 247.

10. L212: Please unify the unit of MEP between the manuscript (mm/y) and the Fig. 3 (mm/a).

Reply: Thanks for your careful work. The unit of “yr” was uniformly used in the Revision to represent “year”.

See Line 251 and the others all through the paper.

11. L214-215: What do you mean “the annual EPF ranged from 1.0 to 2.1”?

Reply: Sorry for my mistake. It should be “mean annual EPF”. We corrected it in the Revision.

Lines 253-254.

12. L316-L306: What do you mean “The streamflow was 2.41/25.6 times of the mean annual streamflow from 2002

to 2011”? What is the meaning of “/” in your manuscript?

Reply: Sorry for my careless. I missed to deleted the characters “/25.6” before submitting. The characters were deleted.

See Line 358.

13. L317-318: Please explain “Therefore, it can be inferred that the EPF obtained in this study, about twice a year on average, is rational” in detail. What do you mean “twice a year”?

Reply: It was corrected as “twice every year”. As mentioned above, the top 5 daily sediment discharge account for 70%-90% of annual sediment discharge. The top 5 daily sediment discharge is generally produced by 1 or 2 EP events every year. The sentence was reworded.

Lines 359-360.

14. L336-338: Why 50 mm/d and 25 mm/d are the suitable threshold for the Southeast and Northwestern of LP, respectively?

Reply: There is no precipitation event exceed 50 mm/d in the northwest Loess Plateau, where mean annual precipitation is <200 mm. However, precipitation events > 50 mm/d often occur in the southeast Loess Plateau. The EPTs determined by universal multifractals are less than 20 mm/d in some stations of the northwest Loess Plateau but > 50 mm/d in some stations of the southeast Loess Plateau. Therefore, our results demonstrated this viewpoint.

The sentences were rephrased.

See Lines 385-388.

15. L358: Please add “the reason” between “may” and “why”

Reply: The phrase was added.

See Line 414.

16. Fig. 3: Please correct the title of the figure. There are 6 subfigures (a-f) in the figure 3. However, only 5 subfigures (a-e) are listed and explained in the title.

Reply: Thanks. Missed information was added.

See Figure 3 in Line 612

## **Comments from Anonymous Referee #2**

In this paper, the authors study observed extreme precipitation in the Loess Plateau in China, derived from 87 meteorological stations in the period 1961 to 2015. They find that while there was a decreasing trend in mean

precipitation in general, the trend in extreme precipitation frequency, intensity, and severity was increasing in parts of the study area. They further find a correlation of extreme precipitation thresholds with soil erosion hazards that regularly happen in this area. They apply multifractal theory and a segmentation algorithm to derive thresholds of extreme precipitation, and state that this method is superior to non-parametric methods that use fixed absolute values or percentiles to define the extreme precipitation threshold. The structure of the paper and the language is clear.

Reply: Thank you very much for your favorite consideration and detailed suggestions. We have studied all the comments carefully and have made corrections.

This analysis in an area that is exposed to hazards related to extreme precipitation is certainly valuable. It further promotes an advanced statistical analysis method based on multifractal theory, that many potential readers are probably not familiar with, including myself. The presentation of the method is at some points confusing, and it has not become entirely clear to me what makes the multifractal method superior to the more common methods from reading the manuscript. I recommend that the authors could improve the manuscript in a major revision, by a better motivation and explanation of the analysis method, and by some additional analysis. In the following, I separate my comments into major and minor points.

Reply: Thanks for your wonderful work.

#### **Major points:**

1. Many readers may be unfamiliar with the theory of multifractals, therefore I recommend to make the explanation in the Methods section somewhat more “didactical”. I understand that it is only possible to provide a very brief outline of the theory in the paper, but I think it might be possible to present the method in a way that allows readers to grasp the general idea, and make them aware of this new method. The more interested reader can then be drawn to book by Lovejoy and Schertzer.

Reply: Thanks for your reminding. The methodology was introduced in more details.

See Lines 106-148.

#### **Here are some specific issues:**

1a) Eq. (1): What would be  $L$  and  $l$  in this specific case of station measurements? Why is  $\lambda$  the density of stations? I thought you apply the method to each station individually, so I would rather expect it is something like the measurement interval?

Reply: Thanks for your detailed comment. I am sorry for my mistake. The  $\lambda$  is the scale ratio of the time series of observed precipitation, and it is indeed the measurement interval as you meant.  $\varphi_\lambda$  is accumulated precipitation at scale  $\lambda$ . Here,  $l$  is the number of the embedded time series at scale  $\lambda$ . For example, for a data series of daily precipitation with length of  $L = 1024$  days, if we defined the measurement scale  $l = 16$  days, then  $\lambda=64$ ,  $\varphi_\lambda$  is the maximum precipitation accumulated at 16 days.

See Lines 106-108.

1b) I don't really understand what "singularity" means in this context. Could you give a simple explanation in your own words, if this is possible in a few sentences? Which values can gamma take?

Reply: The "singularity" means the maximum of precipitation at scale ratio  $\lambda$  in this paper, and generally,  $\gamma_s > 0$ . It was explained in detail in the revision of this manuscript.

See Lines 108, 132-133.

1c) Eq. (3): Is q an integer defining the order of the moment?

Reply: Yes, it was explained in the Revision.

See Lines 112-113.

1d) Similar to 1b: Can you give some more explanation what the multifractal index alpha means? For example, what does it mean if alpha < 1 versus alpha > 1? In Eq. (4) and Eq. (6) it looks like that alpha is written with a "" ("prime"). Is this a typo?

Reply: The multifractal index,  $\alpha$ , quantifies the distance of the process from monofractality. When  $\alpha = 0$ , the process is monofractal, whereas  $\alpha = 2$  means the divergence of data moments. For time series,  $0 < \alpha < 1$ . According to universal multifractal by Tessier et al. (1994) and Lovejoy and Schertzer (2013),  $\alpha'$  is the multifractal index related to  $\alpha$ ,  $1/\alpha + 1/\alpha' = 1$ .

See Lines 117-118.

Lovejoy, S., Schertzer, D., 2013. The weather and Climate: emergent laws and multifractal cascades. Cambridge University Press.

Tessier, Y., Lovejoy, S., Schertzer, D., 1994. Multifractal analysis and simulation of the global meteorological network. Journal of applied meteorology, 33(12): 1572-1586.

1e) l. 135: Is the interval space d a parameter? How is it selected?

Reply: The parameter  $d$  is an interval that was used to gradually remove extremes in the EPT determining procedure, and the  $d$  was set 1 mm/d.

See Line 160.

1f) Eq. (7): Define and explain  $\mu_L$ ,  $\mu_R$ ,  $s_D$ .

Reply: The parameters  $\mu_L$ ,  $\mu_R$ , and  $s_D$  were defined.

See Lines 167-168.

1g) Eq. (8): Should it be P(tau) instead of P(t) here? Otherwise I don't understand the meaning of this equation.

Reply: Yes, thanks for your careful work. The parameter was corrected as you noted.

See Lines 168, 171.

2. The trend calculation in section 4.3 is certainly an important result of your paper. Therefore, I strongly recommend to perform significant tests for ALL indices shown in Fig. 4, including the mean precipitation. Why did you use significance level  $p < 0.1$  for EPI, and  $p < 0.05$  for EPS? It would be better to use the same significance level for all indices. It would also be good to mark regions with significant trends in all panels. One possibility would be to mark all stations with positive significant trends with blue dots, all stations with negative significant trends with red dots, and all stations with insignificant trends with black dots.

Reply: According to this comment, Figure 4 was replotted, and stations with significant trends were marked. To show more stations with higher trends, the significance level of 0.1 was selected. Information about significant trends of individual indices were added.

See Figure 4, Lines 273-274, 278-279.

3. I think the claim that the multifractal method is superior to the more common analysis methods it is not yet clearly justified. There should be a direct comparison of the non-parametric methods with the multifractal method, especially for the results shown in section 5.2. In Fig. 8, can you add a panel with the EPTs calculated from the multifractal method, and explain the differences to the others? The "standard deviation method" shown in panel 8f comes out of nowhere, please define it. It is not explained anywhere yet. Could you also show the goodness-of-fit numbers for the EP distributions from the multifractal results, and compare them to the non-parametric methods shown in Fig. 9? You could mark them in the panels in Fig. 9, or list them in a table.

Reply: A figure for EPT determined by multifractal method was added in Figure 8. The 3-times standard deviation method was briefly introduced. The goodness-of-fit of EP events determined by universal multifractals in individual stations show good passing rates, 100%, and the Table 2 was added to list these results. In addition, the functions always with low passing rates are inappropriate for the analysis. Accordingly, we have replaced the parameter functions with low passing rate by those with high passing rates, including Pearson type III, generalized normal distribution.

See Lines 383-385, Table 2, 423-425.

#### **Minor points:**

4. Definition of the EP indices (Section 2.3): The abundance of symbols is confusing here. The EP severity EPS is called EPSI in Table 1, Fig. 3f, and probably other places. Please use the same acronyms everywhere. It is also confusing that EPI and EPT are called  $P_I$  and  $P_T$ , respectively, in Eq. (9). Better use EPI and EPT in Eq. (9). In Eq. (11),  $P_F$  is not defined. It is the same as EPF, I assume, so you can also better use EPF here.

Reply: Sorry for my carelessness. The acronym of EP severity was uniformly defined as EPS in the Revision. According to this comment, these parameters used in Eqs. (9) and (11) were replaced by their acronyms.

See Equation (13) in line 185, and Table 1.

5. Eq (11): How sensitive are the results for EPS to the choice of  $k_1$  and  $k_2$ ? (See Fig. 3f, Fig. 4e)

Reply: Yes, the EPS is the combination of both EPF and EPI, and the results for EPS is sensitive to the choice of  $k_1$  and  $k_2$ . Accordingly, the choice of the values of  $k_1$  and  $k_2$  is strictly according to studies reported by IPCC (2007).

See Line 202.

6. 1. 84/85: "For precipitation, a scaling break ... roughly two weeks." What does this sentence mean? Could you be more precise?

Reply: Studies of the scaling property of precipitation using multifractals showed that the scaling break of precipitation at a station does not always equal to those from the other stations around the world. Generally, the scaling break ranges from several days to about 1 month around the world, with an average about 2 weeks. This information was added.

See Line 89.

7. The index EP as shown in Fig. 4b is not given in Table 1. Or do you mean MEP here?

Reply: MEP is mean annual EP; it is used in spatial variation presentation of EP over the past 55 years. Figure 4b shows the trends of annual EP in spatial.

8. 1. 236: "... the annual EPF changed by -0.6 to +0.5 days,..." Where are these numbers from? They are not given in the figure. Is this the total trend for the whole time series?

Reply: Yes, the "-0.6 to +0.5 days" were total changes of EPF over the past 55 years. These were calculated by multiplying slopes by years. Information was added.

See Line 278.

9. 1. 273: "According to the average sea level pressure and winds at the 1000 hpa level..." This does not seem to make sense. Either you can give the air pressure at a given height level, or the geopotential height at a given pressure level.

Reply: Thanks for your reminding. we deleted "at the 1000 hpa level".

See Line 316.

10. 1. 334/335: "It can be seen... lower percentiles". This seems trivial. Either remove this sentence, or write something like: "Trivially, thresholds are smaller..."

Reply: The sentence was rewritten as this comment suggested.

See Lines 382-383.

11. Figs. 3 and 4: Why are there different station names shown in different panels? For example, the Xiji station is mentioned in connection with panel 4e, but it is not shown in this panel. So one has to find it in one of the other panels.

Reply: These labels had been listed to describe the regions with different values or trends. According to this comment, we replotted Figures 3 and 4 to list same station labels in all these figures.

As shown in Figures 3 and 4.

12. The tropical cyclone situation shown in Fig. 6c and 6d: Do these maps show mean fields for the whole day, or an instantaneous situation?

Reply: Yes, these maps show mean fields for the whole day. This information was added.

See Line 622.

### **Small corrections:**

l. 19: "scarce" (instead of "scare")

Reply: The word was corrected.

See Line 20.

l. 167: "1" should be subscript in "k1".

Reply: We corrected it.

See line 202.

l. 193: There is no Fig. 2b

Reply: The figure should be Fig. 2. We corrected it.

See Line 231.

l. 194: Link is not accessible to me.

Reply: The website was changed to be <http://data.cma.cn/>. It was revised.

See Line 232.

l. 255: "... and EPS had a negative \*trend in\* annual..." and in the following line "... LP area with negative \*trend in\* annual..."

Reply: Thanks. The sentences were corrected.

See Lines 298-300.

l. 332: "...parametric and non-parametric..."

Reply: Sorry for my carelessness. The two words were corrected.

See Line 380.

## **Comments from Anonymous Referee #3**

This paper suggests a novel approach to assess spatio-temporal extremes of precipitations and implements it over of the Loess Plateau of China. The topic is interesting and relevant for the community. The data used seems of quality. The framework of Universal Multifractals (UM) is appropriate for such an issue. However I would not recommend to publish this paper in its current state, mainly for methodological reasons.

Reply: Thank you for your attention reviewing our manuscript.

Indeed the methodology developed to determine the EPT(section 2.2) seems to contradict the underlying ideas of a multifractal framework. If I understood well the suggested methodology, it consists in performing UM analysis on the series after removing more and more extremes (replacing them with which values ?). Then the retrieved parameters are analysed and a so called “physically meaningful” threshold determined.

Reply: the eliminated “extremes” were replaced by zeros in the procedure of EPT determination.

I have trouble understanding the logic behind this choice. Indeed, the interest of UM analysis is to analyse the whole data available and obtain  $K(q)$  and  $c(\gamma)$  which then fully characterize the variability across scales. Removing the extremes will simply degrade the quality of the scaling (hence the reliability of the estimates), bias the analysis, and not improve the knowledge on the studied series. EP should be derived directly from the co-dimension function or scaling moment function obtained on the best data available.  $\gamma_s$  could actually be a good choice, but other could be developed notably to include notion of both intensity and frequency as suggested by the authors. Since all the following depends on the the indicators obtained from this methodology, I believe that this methodology should either more justified (I may have miss a point) or updated before any further study.

Reply: It is sure that the multifractal representation captures the observations independently of when or how extreme precipitation came to be. In this way, the UM can be applied to infer the magnitude of precipitation maximum within a return period, and more precise results can be obtained in comparison with traditional parameter functions, see Douglas and Barros (2003). The first author had also applied the UM to estimate maximum precipitation with a duration in his doctoral dissertation, as shown in the Figure below. However, such an estimation of maximum precipitation within a duration has nothing to do with spatiotemporal EP variation assessment over a long period in a large area.

In universal multifractals analysis, the codimension function  $c(\gamma)$  characterizes the sparseness of the  $\gamma$ -order singularities (maximum). The parameter  $\gamma_s$  represents the maximum of accumulated precipitation ( $\varphi_s$ ) at the scale ratio  $\lambda$  (Douglas and Barros, 2003; Lovejoy and Schertzer, 2013; Tessier et al., 1994). Therefore,  $c(\gamma)$  and  $\gamma_s$  naturally capture the statistical properties of extremes of a data set. If we gradually eliminate extreme precipitation (EP) (replacing extremes by zeros), these exponents or functions will change and will sharply change if majority of the extremes are removed, because singularity largely depend on extremes; and those abrupt points can be determined as extreme precipitation threshold (EPT). This is the theoretical basis for EPT determination, as shown

in Figure 1 of the manuscript. However, the procedure determining EPT does not give rise to any bias, because all the following analyses are based on original data. Therefore, the methods in this study will not result in quality degradation etc., as it was concerned in this comment.

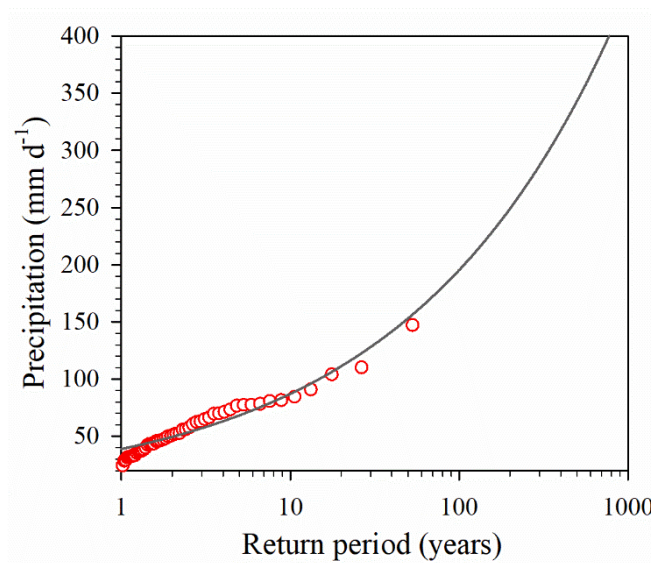


Figure 1. Projected extreme values as a function of their return period.

Douglas, E.M., Barros, A.P., 2003. Probable maximum precipitation estimation using multifractals: application in the Eastern United States. *Journal of Hydrometeorology*, 4(6): 1012-1024.

Lovejoy, S., Schertzer, D., 2013. *The weather and Climate: emergent laws and multifractal cascades*. Cambridge University Press.

Tessier, Y., Lovejoy, S., Schertzer, D., 1994. Multifractal analysis and simulation of the global meteorological network. *Journal of applied meteorology*, 33(12): 1572-1586.

In addition, indication of the quality of the scaling, and scaling curves should be provided to the reader.

Reply: One of the aims in this paper is to propose a method to determine EPT using multifractal technique. The scaling properties of precipitation, runoff etc., were widely explored using multifractal methods in the past 15 years. There are many papers can be referred. For clarification, the methodology was introduced in more detail.

See Lines 106-178.

## **Short Comments from Zhihua Shi**

### **General comment**

In this work the authors proposed an approach integrating the universal multifractals and a segmentation algorithm

to precisely identify EP events. Then they assessed spatiotemporal variation of extreme precipitation over the Loess Plateau, China. It is known that extreme precipitation in the Loess Plateau is one of the major agents causing serious environment hazards in the Loess Plateau. However, to my knowledge, traditional method including parameter methods and non-parameter method could not give such a rational result of extreme precipitation in both spatial and temporal distribution. The method proposed in this paper is innovative, and the results are of great significance in catchment management. The paper is in good presentation and fluent expression, and the content of the paper suits to HESS.

Reply: Thanks a lot for your favorite consideration and detailed suggestions. We have studied all the comments carefully and have made corrections.

**My detailed comments follow:**

1. The authors should describe the procedure to calculate the EP indices in detail.

Reply: Procedure to calculate individual EP indices was added.

See Lines 180-205.

2. Can the methodology proposed in this paper be applied to extreme precipitation assessment in many other regions? Please discuss this point at the end of the abstract.

Reply: Yes, the method can be applied to regional EP assessment in many other regions, it was introduced at the end of the abstract.

See Lines 28-29.

3. Line 42: The most serious soil erosion in the Loess Plateau should be  $3 \times 10^4 - 4 \times 10^4 \text{ t} \cdot \text{km}^{-2} \cdot \text{yr}^{-1}$ . Please check it.

Reply: Thanks for your reminding. The data was corrected.

See Line 43.

4. Line 153: The abbreviation of “EP severity (EPS)” doesn’t agree with “EPSI” in Table 1. Please check it throughout the paper.

Reply: Thanks for your reminding. The EP severity was uniformly abbreviated as EPS in the Revision.

See Line 189, Table 1 and the others all through the paper.

5. Line 215: Add the unit to the annual EPF.

Reply: Thanks for your reminding. The unit was added.

See Line 254.

6. Line 231: it should be “4.2 Spatiotemporal variation of EP”.

Reply: Thanks. The number of the section title was corrected.

See Line 272.

7. Line 238: It should be “mainly in”

Reply: Thanks. The word was corrected.

See Line 281.

8. Please check the units used throughout the paper and make sure each unit is strictly unique in the paper. For example, Line 42 “yr<sup>-1</sup>”, Line 214 “days” and Line 237 “days/yr” don’t in consistent with “d” and “d/yr” used in Figures 3 and 4.

Reply: We have checked all units used in the paper and made correction. The unit “d” and “yr” were adopted to represent day and year, respectively. Figures 3 and 4 was replotted and the units were corrected. Besides, units in the form of superscript negative powers instead of divided by positive powers were adopted all through the paper.

See Figure3 3 and 4.

9. The scarce precipitation but intense EP is a major external agent inducing most serious sediment erosion in Loess Plateau. The spatial EPI and EPS derived in this paper is important as it well illustrate this question. This is an important question should be further discussed in section 5.1.

Reply: Thanks for your suggestion. We have enlarged discussion in section 5.1 about EP events and their corresponding natural hazards including sediment erosion.

See Lines 362-372.

10. There are some studies to explore the EP in the Loess Plateau. The authors should compare their results with previous studies.

Reply: Further discussed was added in 5.2.

See Lines 411-415.

# A Universal Multifractal Approach to Assessment of Spatiotemporal Extreme Precipitation over the Loess Plateau of China

Jianjun Zhang<sup>1, 2, 5</sup>, Guangyao Gao<sup>2</sup>, Bojie Fu<sup>2</sup>, Cong Wang<sup>2</sup>, Hoshin V. Gupta<sup>3</sup>, Xiaoping Zhang<sup>4</sup> and Rui Li<sup>4</sup>

5 <sup>1</sup>School of Land Science and Technology, China University of Geosciences, Beijing 100083, China

<sup>2</sup>State Key Laboratory of Urban and Regional Ecology, Research Center for Eco-Environmental Sciences, Chinese Academy of Sciences, Beijing 100085, China

<sup>3</sup>Department of Hydrology and Atmospheric Sciences, The University of Arizona, Tucson, AZ 85721, USA

10 <sup>4</sup>State Key Laboratory of Soil Erosion and Dryland Farming on the Loess Plateau, Institute of Soil and Water Conservation, Chinese Academy of Sciences and Ministry of Water Resources, Yang ling, Shaanxi, 712100, China

<sup>5</sup>Key Laboratory of Land Consolidation and Rehabilitation, Ministry of Natural Resources, Beijing 100035, China

*Correspondence to:* Hoshin V. Gupta (hoshin@email.arizona.edu)

**Abstract.** Extreme precipitation (EP) is a major external agent driving various natural hazards in the Loess Plateau (LP), China. Yet, the characteristics of spatiotemporal EP responsible for such hazardous situations remain poorly understood. We integrate  
15 universal multifractals with a segmentation algorithm to characterize a physically meaningful threshold for EP (EPT). Using daily data from 1961 to 2015, we investigate the spatiotemporal variation of EP over the LP. Our results indicate that, with precipitation increasing, EPTs range from 17.3 to 50.3 mm<sub>d<sup>-1</sup></sub> while the mean annual EP increases from 35 to 138 mm from northwest to southeast LP. Further, EP frequency (EPF) has historically spatially varied from 54–116 days, with the highest EPF occurring in the mid-southern and southeastern LP where precipitation is much more abundant. However, EP intensities  
20 tend to be strongest in the central LP where precipitation also tends to be scarce, and get progressively weaker as we move towards the margins (similarly with EP severity). An examination of atmosphere circulation patterns indicates that the central LP is the boundary where tropical cyclones reach furthest into inland China, resulting in the highest EP intensities and EP severities being in this area. Under the control of the East Asian monsoon, precipitation from June to September accounts for 72% of the total amount, while 91% of the total EP events are concentrated in June to August. Further, EP events occur, on  
25 average, 11 days earlier than the wettest part of the season. These phenomena are responsible for the most serious natural hazards in the LP, especially in the Central region. Spatiotemporally, 91.4% of the LP has experienced a downward trend of precipitation, while 62.1% of the area has experienced upward trends of the EP indices, indicating the potential risk of more serious hazardous situations. The universal multifractal approach considers the physical processes and probability distribution of precipitation, thereby providing a formal framework for spatiotemporal EP assessment at regional scale.

## 30 1. Introduction

Extreme precipitation (EP) is the dominant external agent driving floods, erosion, and debris flow etc., with adverse impacts on human life, the social economy, the natural environment, and ecosystems (Min et al., 2011; Pecl et al., 2017; Walther et al., 2002). These impacts are especially severe in arid and semiarid areas because of the sparsity of vegetation and fragility of the eco-environment (Bao et al., 2017; Huang et al., 2016). In recent decades, worldwide climate change has given rise to spatially  
35 heterogeneous changes in EP regime (Donat et al., 2016; Manola et al., 2018; Zheng et al., 2015). Such uneven changes in EP have the potential to aggravate adverse impacts on human life and eco-environment and, consequently, EP has recently received increased attention (Eekhout et al., 2018; Li et al., 2017; Wang et al., 2017). In this regard, a fundamental need is to evaluate the regional spatiotemporal variation of EP, providing important information that is crucial to natural resource management and sustainable social development.

40 The Loess Plateau (LP), which is located in the middle reaches of the Yellow River, is a typical arid and semiarid region, characterized by serious EP-induced natural hazards, including soil erosion and consequent hyper-concentrated flooding and occasional landslides, etc. (Cai, 2001). In the LP area, EP-induced soil erosion generates some of the highest sediment yields observed on earth, ranging from  $3 \times 10^3$  to  $4 \times 10^4$  t·km<sup>-2</sup>·yr<sup>-1</sup>. For example, sediment delivered to the Yellow River in recent decades was estimated to be  $16 \times 10^8$  t·yr<sup>-1</sup> (Ran et al., 2000; Tang, 2004), and sediment deposition resulted in the river  
45 bed of the lower Yellow River aggrading by 8–10 m above the surrounding floodplain (Shi and Shao, 2000). As it flows on the aggraded thalweg, the extreme-precipitation-driven hyper-concentrated floodwaters cause, in turn, the lower Yellow River to burst its channel. Over the past 2500 years, this has caused flooding 1,593 times, and changes to the course of the river channel 26 times, leading to unimaginable death and devastation (Ren, 2006; Tang, 2004). To control such EP induced natural hazards, ecological restoration projects have been implemented over the LP. For example, the “Grain for Green” project (the  
50 largest investment project in China) was implemented to control natural hazards such as soil erosion and flooding, and has cost more than 75 billion dollars over the past 20 years.

Accordingly, a better understanding of spatiotemporal EP changes in this area is of considerable interest for various fields, such as risk estimation, land management, flood control, and infrastructure planning (Feng et al., 2016; Wang et al., 2015). Considerable past work has been devoted to investigating the spatiotemporal variation of total precipitation and precipitation  
55 extremes in this region, with consensus obtained for precipitation “amount” (Li et al., 2010a; Li et al., 2010b; Miao et al., 2016; Wan et al., 2014; Xin et al., 2009). However, the spatial distribution of EP in the LP is still poorly understood, with considerable disagreement regarding EP and the inability to account for the spatial distribution of EP-induced hazards such as soil erosion (Li et al., 2010a; Li et al., 2010b; Miao et al., 2016; Wan et al., 2014; Xin et al., 2009). It is therefore important to account for the spatiotemporal role of EP in natural hazards, to facilitate better catchment management in regards to issues such as  
60 freshwater shortage (Feng et al., 2012).

To understand spatiotemporal variations in EP, scientists are often required to collect more detailed data, including maximum depth, duration, and area observations (Dulière et al., 2011; Herold et al., 2017; Miao et al., 2016). Despite sophisticated methodologies, such efforts rely on data from various sources, which are typically absent in the long-term historical observational records, especially over large areas. Therefore, any investigation of spatiotemporal variation in EP must make use of the information in available historical data that was observed at fixed time intervals (e.g. daily). In EP assessment using historical daily data, it is a crucial step to identify EP events by extreme precipitation threshold (EPT) determination. However, EP events tend to be relatively rare, unpredictable, and often of short duration (Liu et al., 2013), and this uncertainty, combined with varying geographical and meteorological conditions, increases the complexity of EP assessment.

In general, existing methods for EPT determination can be grouped into two categories: nonparametric and parametric. Non-parametric methods use fixed critical values or percentiles to define the thresholds for extreme events. Because the corresponding classification of EPTs varies from region to region (e.g., a 50 mm daily precipitation event is considered normal in South China but would be an EP event in the LP), the application of non-parametric methods can require considerable subjectivity (Liu et al., 2013), and significantly affect the results of the analysis. For instance, using an absolute value of 50 mm/d, Xin et al. (2009) reported a spatiotemporal decreasing zone of EP in mid-eastern LP while, using the 95% percentile to determine EP, Li et al. (2010a) and Li et al. (2010b) found an increasing trend of EP frequency in the southeastern LP. These reports did not, however, explain the rationale for spatial variation of EP and its impacts on the most serious soil erosion in the central LP.

Parametric statistical methods based on empirical distributions have recently become popular. A variety of special distribution functions and parameter estimation techniques have been proposed to characterize observed EP (Anagnostopoulou and Tolika, 2012; Beguería et al., 2009; Deidda and Puliga, 2006; Dong et al., 2011; Li et al., 2005; Pfahl et al., 2017). A recent focus that has emerged is to obtain better physical understanding of EPTs, and thereby to assess regional variations in EP. For example, Liu et al. (2013) adopted a multifractal detrended fluctuation analysis (MFDFA) to determine EPTs, and Du et al. (2013) applied MFDFA to investigate EPTs and consequent EP variation in Northeastern China. To date, however, no international standards for the selection of such methods exist.

Recent investigations of precipitation using the universal multifractal technique have demonstrated its multifractal nature. Universal multifractals were conceived to study the multiplying cascades governing dynamics of various geophysical fields (Lovejoy and Schertzer, 2013; Schertzer and Lovejoy, 1987). For precipitation, a scaling break separates the meteorological and climatological regimes varies from several days to 1 month, with an average about ~~at roughly~~ two weeks (Tessier et al., 1996; Tessier et al., 1994, 1993). The meteorological scaling interval indicates that, from the multifractal perspective, data collected at time intervals of one day and those at intervals finer than minutes can equivalently characterize the physical processes associated with precipitation (Pandey et al., 1998; Tessier et al., 1996), indicating that EP events can, in principle,

be characterized by the study of daily data observed at gauging stations. Of course, it is vitally important that the universal multifractal characterizes how extremes occur in a natural manner (Lovejoy and Schertzer, 2007; Tessier et al., 1996).

95 In this study, we use the universal multifractal technique to obtain a physically meaningful characterization of EPT. Our objectives are to (1) apply the universal multifractal approach to determine a unique set of EPTs for the LP area, (2) investigate how spatial variations in EP are responsible for the severe nature of soil erosion, and (3) assess the spatiotemporal variation of EP over the LP during the period 1961-2015.

## 2 Methodology

### 100 2.1 The relationship between precipitation extremes and Multifractals

The approach outlined below was used to identify EP events at the observation time scale. In the method of universal multifractals, two equivalent routes can be followed to investigate time series scaling: the probability distribution and the statistical moments. A fundamental property of multifractal fields related to the probability distribution is given by the equation (Lovejoy and Schertzer, 2013; Schertzer and Lovejoy, 1987):

$$105 \quad \Pr(\varphi_\lambda > \lambda^\gamma) \approx \lambda^{-c(\gamma)} \quad (1)$$

where  $\lambda$  represents the resolution of the measure (i.e., the ratio of the external scale  $L$  to the measurement scale  $l$ ;  $\lambda = L/l$ ),  $\varphi_\lambda$  is the intensity of the field (in this case accumulated precipitation) measured at resolution  $\lambda$  ~~(in this case the density of stations)~~,  $\gamma$  is the order of singularity (maximum precipitation) corresponding to  $\varphi_\lambda$ , and the codimension function  $c(\gamma)$  characterizes the sparseness of the  $\gamma$ -order singularities (this function is a basic multifractal probability relation for cascades). Accordingly, the  
110 statistical moments are given by

$$\langle \varphi_\lambda^q \rangle = \lambda^{K(q)} \quad \lambda > 1 \quad (2)$$

where  $K(q)$  is the multiple scaling exponent function for moments—;  $q$  is the order of the statistical moment and  $\langle \rangle$  denotes the average of the field (averaged precipitation) at scale ratio  $\lambda$ . The two equivalent routes are related via a Legendre transform (Parisi and Frisch, 1985). The universal  $K(q)$  functions and the codimension function  $c(\gamma)$  are expressed as

$$115 \quad K(q) = \begin{cases} \frac{C_1}{\alpha - 1} (q^\alpha - q) & \alpha \neq 1 \\ C_1 q \log(q) & \alpha = 1 \end{cases} \quad (3)$$

$$c(\gamma) = \begin{cases} C_1 \left( \frac{\gamma}{C_1 \alpha'} + \frac{1}{\alpha} \right)^{\alpha'} & \alpha \neq 1 \\ C_1 \exp\left(\frac{\gamma}{C_1} - 1\right) & \alpha = 1 \end{cases} \quad (4)$$

where  $0 \leq \alpha \leq 2$  is the multifractal index, which describes how rapidly the fractal dimensions vary as we leave the mean. For time series in this paper,  $0 < \alpha < 1$ , and  $\alpha'$  is the auxiliary variable defined by  $1/\alpha' + 1/\alpha = 1$  (Lovejoy and Schertzer, 2013).

120 The term  $C_1$ , the codimension of the mean of the process, varies on  $0 \leq C_1 \leq D$  ( $D$  is space dimension;  $D = 1$  for time series) and quantifies the sparseness of the mean. In this paper, the parameters  $\alpha$  and  $C_1$  of the multifractal model were estimated using the double trace moment technique (Lavallée et al., 1993).

As noted by Gagnon et al. (2006) and Lovejoy and Schertzer (2007), the parameters  $C_1$  and  $\alpha$  characterize the mean of the field, whereas the extremes are expressed by the singularity,  $\gamma$ , and the codimension function  $c(\gamma)$  (Hubert et al., 1993). For  $0 \leq \alpha < 1$  and considering a time series of infinite length, a finite maximum order of singularity,  $\gamma_0$ , can be determined as

$$125 \quad \gamma_0 = \frac{C_1}{1-\alpha} \quad (5)$$

However, in general, any time series of finite length will almost surely miss the presence of rare extremes in the field. In this case, the observed singularities will be bounded by an effective maximum singularity,  $\gamma_s$ :

$$\gamma_s = \gamma_0 \left[ 1 - \alpha \left( \frac{C_1}{D} \right)^{-1/\alpha'} \right] < \gamma_0 \quad (6)$$

130 where  $D$  is the embedding space dimension ( $D=1$  for the time series). The total dimension of this problem is actually  $(D+D_s)$ , where  $D_s = \log N_s / \log \lambda$  is the sampling dimension, and  $N_s$  is the number of independent time series at each location. The parameter  $\gamma_s$  links the physical processes that generate precipitation events to the conceptual model of multiplicative cascades, and allows the extremes to be cast in a probabilistic framework,  $\gamma_s > 0$ . Thus, it was used to infer the extreme events of precipitation fields over well-defined ranges of scale.

135 For parameter estimation, the parameters  $\alpha$  and  $C_1$  of the multifractal model are estimated by the double trace moment (DTM) technique (Lavallée et al., 1993). The  $q, \eta$  DTM at resolution  $\lambda$  and  $\Lambda$  is defined as

$$Tr_\lambda (\phi_\Lambda^\eta)^q = \left\langle \sum_i \left( \int_{B_{\lambda,i}} \phi_\Lambda^\eta d^D x \right)^q \right\rangle \propto \lambda^{K(q,\eta) - (q-1)D} \quad (7)$$

where the sum is obtained over all the disjoint  $D$  dimensional balls  $B_{\lambda,j}$  (with intervals of length  $\tau = T/\lambda$ ) that are required to cover the time series.  $K(q,\eta)$  is the double trace scaling exponent, and  $K(q,1) = K(q)$  is the scaling exponent. This relation can be expressed as

$$140 \quad \left\langle \left( \varphi_{\lambda}^{\eta} \right)_{\lambda}^q \right\rangle = \lambda^{K(q,\eta)} \quad (8)$$

where the notation indicates that the multifractal  $\varphi$  at a (finest) resolution  $\Lambda$  is first raised to the power  $\eta$  then degraded to resolution  $\lambda$ , and the  $q$ th power of the result is averaged over the available data. The scaling exponent  $K(q,\eta)$  is related to  $K(q,1) \equiv K(q)$  and given by

$$K(q,\eta) = K(q\eta - 1) - qK(\eta,1) \quad (9)$$

145 In the case of universal multifractals, by plugging Eq. (3) into Eq. (5),  $K(q,\eta)$  has a particularly simple dependence on  $\eta$ :

$$K(q,\eta) = \eta^{\alpha} K(q) \quad (10)$$

where  $\alpha$  can be estimated from a simple plot of  $K(q,\eta)$  versus  $\log(\eta)$  for fixed  $q$ . Thus, based on DTM technique, all parameters can be estimated.

## 2.2 Determination of the extreme precipitation threshold

150 The approach outlined below was used to estimate the EPTs and EP events for each station, using the singularity parameter,  $\gamma_s$ . Given that the multifractal parameters  $\alpha$  and  $\gamma_s$  naturally characterize extremes, both of these parameters will change if we gradually remove extreme values from the data set. The singularity of the precipitation data series will be completely changed, and the two parameters will significantly change if all of the extreme values are deleted. To obtain a physically meaningful value for the EPT, we attempted to estimate the multifractal parameter series by applying the universal multifractal approach

155 to our precipitation series and successively eliminating maximum values of precipitation. However, as shown by Figures 1a and 1c, the degree of convergence to the original value is not unique, with the values fluctuating slightly around the original  $\alpha$  and  $\gamma_s$ . Accordingly, the variance series of index series  $\alpha_j$  and  $\gamma_{s,j}$  were computed to eliminate the fluctuation while identifying the point of convergence. The procedure is as follows:

- 160 1) Eliminate the data point  $x_j, \{x_j, x_j \geq x_{\max} - d \times j\}$  from the precipitation time series  $\{x_i, i = 1, 2, \dots, n\}$ , where  $x_{\max}$  is the maximum,  $x_{\text{ave}}$  is the average, and  $d$  is the interval space (we set  $d = 1$  mm in this case).
- 2) Compute the selected parameters.
- 3) Repeat (1) and (2) for  $j$  varying from 1 to  $\text{int}((x_{\max} - x_{\text{ave}})/d)$ .

Using the obtained parameter series, we applied the segmentation algorithm proposed by Bernaola Galván et al. (2001) to determine the point of abrupt change, which we define as the EPT. The segmentation algorithm is based on the calculation of the statistic  $t$  of each data point in a series or subseries:

$$\tau = \left| (\mu_L - \mu_R) / s_D \right| \quad (711)$$

where  $s_D = [(s_L^2 + s_R^2) / (N_L + N_R - 2)]^{1/2} (1 / N_L + 1 / N_R)^{1/2}$  is the pooled variance. The  $\mu_L/\mu_R$ ,  $s_L/s_R$ , and  $N_L/N_R$  are the mean, standard deviation, and number of points from the data to the left/right of the series, respectively. The significance level  $P(\neq \tau)$  of the largest value  $t_{\max}$  obtained from Eq. (711) is defined as the probability of obtaining a value equal to or less than  $\tau$  within a random sequence (Swendsen and Wang, 1987)

$$P(\tau) = \Pr \{ t_{\max} \leq \tau \} \quad (812)$$

If the significance exceeds a selected threshold  $P_0$  (usually taken to be 95%), an abrupt point is selected and the series is cut at this point into two subsets.

The pooled variances and the abrupt points of the  $\alpha$  and  $\gamma_s$  series are shown in Figures 1b-1d. The abrupt point, where  $s_D$  differs from its left-side points but is approximately equal to its right-side points, is selected to be the EPT. As shown in Figure 1, for the determined EPT, there are a deep slope of the pooled variance on the left while a gentle slope on the right of daily precipitation 37.1 mm. Thus, the EPT for Xingxian station is estimated as 37.1 mm/d, and 90 EP events have occurred over the past 55 years (Figure 1c).

### 2.3 EP indices

All of the variables characterizing spatiotemporal EP over the LP are shown in Table 1. For individual station, annual precipitation at each station was accumulated using daily data. Annual EP is accumulated using daily EP determined by EPT, and EP frequency (EPF) is the number of daily EP events. Mean annual EP (MEP) is averaged from annual EP interpolated using ArcGis 10.1. For a year with  $n$  EP events, EP intensity (EPI) is calculated by the equation~~The crucial variable, EPT and the mean annual EP (MEP) are presented to provide a general description of EP.~~

$$EPI = \frac{1}{n} \sum_{i=1}^n (EP_i - EPT) / EPT, \quad i = 1, 2, \dots, n. \quad (13)$$

where  $EP_i$  represents the magnitude of EP event  $i$ , respectively.

As noted by IPCC (2007), ~~the severity of EP (EPS) events relies on both intensity and frequency. Neither~~ the cases of high frequency with low intensity, or low frequency with high intensity, can reflect the severity of EP events given a long-term time series for an area-, while the severity of EP (EPS) events relies on both intensity and frequency. Consequently, we examine

190 the extreme precipitation intensity (EPI), extreme precipitation frequency (EPF, defined below) and EPS to characterize the spatiotemporal nature of EP over the LP. ~~In addition, we compute the mean daily precipitation (MDP) and the accumulated daily EP events (ADEP) to help characterize the intra-annual precipitation and EP.~~

~~The EPF at a station is the number of days exceeding EPT. Annual values of EPI ( $P_i$ ) for a station are given by~~

$$\text{EPI} = \frac{1}{n} \sum_{i=1}^n (EP_i - EPT) / EPT, i = 1, 2, \dots, n. \quad (9)$$

195 ~~where  $P_i$  and  $PE$  represent EPT and the magnitude of EP, respectively.~~ To obtain the concordant EPS, each annual EPF/EPI series is standardized to the range 0 to 1 using equation (10):

$$X = (X_i - X_{\min}) / (X_{\max} - X_{\min}) \quad (10)$$

where  $X_{\min}$  and  $X_{\max}$  represent the lowest and highest annual EP frequency/intensity, respectively. The annual EPS for each station ( $0 \leq \text{EPS} \leq 1$ ) is calculated from the standardized  ~~$P_i$ -EPI~~ and  ~~$P_i$ -EPF~~ by

200 
$$\text{EPS} = k_1 P_i + k_2 P_f \quad (11)$$

where  $k_1$  and  $k_2$  are the weight coefficients of frequency and intensity influencing EP severity, respectively, and  $k_1 + k_2 = 1$ . In this paper,  $k_1$  and  $k_2$  are set 0.5, ~~as both EPI and EPF play major roles in the EPS of EP events according to [IPCC, (2007)].~~

~~In addition, we compute the long-term mean daily precipitation (MDP) and the long-term accumulated daily EP events (ADEP) to help characterize the intra-annual precipitation and EP. As shown in Table 1, MDP is averaged from all 87 stations, and~~  
 205 ~~ADEP is accumulated from 87 stations over the past 55 years.~~

## 2.4 Spatiotemporal EP presentation

The spatial distributions of the EP indices were derived by interpolation via Kriging (Oliver and Webster, 1990), using data observed at the gauging stations. All spatial ~~analysis-analyses~~ were carried out using the ArcGis 10.1 software. Spatiotemporal trends for annual EP ~~variables-indices~~ were computed for each pixel using the least squares method. Following Stow et al.  
 210 (2003), the trend is defined as the slope of the least squares line that fits the inter-annual variability of individual EP indices during the study period, given by:

$$S = \frac{m \times \sum_{j=1}^m (j \times P_j) - \left( \sum_{j=1}^m j \right) \left( \sum_{j=1}^m P_j \right)}{m \times \sum_{j=1}^m j^2 - \left( \sum_{j=1}^m j \right)^2} \quad (12)$$

where  ~~$n$~~  $m$  is the total of years,  $P_j$  is value of the pixel in the  $j$ -th year.

### 3. Study area and database

#### 215 3.1 Study area

The LP (640 000 km<sup>2</sup>) is a typical arid and semiarid area located in the middle reaches of the Yellow River (750 000 km<sup>2</sup>) and characterized by a continental monsoon climate. Elevations range from 84 m to 5207 m (Figure 2). The desert-steppe, typical steppe, and forest steppe (deciduous broad-leaf forest) zones are distributed from northwest to southeast, and correspond to mean annual isohyets of 250, 450, and 550 mm in the arid, semiarid, and semi-humid areas, respectively. The continuous loess covering ranges from 100 m to 300 m in thickness on the mountains, hills, basins, and alluvial plains of different heights. The northwestern part of the region is dominated by flat sandy areas. The middle and southeastern parts are characterized by EP induced water-erosion landform (Zhang et al., 1997), with a rugged undulating ground surface that is broken, barren, and dissected by gullies and ravines (Cai, 2001). EP-induced flooding episodes occur occasionally in the summer, with sediment concentrations generally exceeding 300 kg/m<sup>3</sup> and have been observed to be as large as 1,240 kg/m<sup>3</sup>. The hyper-concentrated flooding has historically resulted in numerous disasters, with severe consequences to people and livestock (Zhang et al., 2017). The amount of soil erosion has been estimated to be larger than 2000 to 3000 million tons per year (Tang, 1990). Soil erosion has resulted in the density of gullies and ravines in the LP being larger than 3–4 km/km<sup>2</sup>, with the maximum exceeding 10 km/km<sup>2</sup>.

#### 3.2 Database

230 To conduct the EP assessment, we used daily data available for 87 national meteorological stations in and around the LP (Figure 2b), consisting of continuous time series from 1961 to 2015. All the precipitation data were obtained from the China Meteorological Data Sharing Service System (<http://data.cma.cn/http://cdc.nmic.cn/home.do>). Missing data accounted for < 0.1% of total sample, and were replaced by a value of 0 in this paper; this replacement of a very few missing values does not influence the analysis. Data regarding severity of soil erosion were provided by the LP Science Data Centre of the Data Sharing Infrastructure of Earth System Science of China (<http://loess.geodata.cn>). These data were compiled during the Soil Erosion Census of the First National Water Conservancy Census (2014). Mean annual vegetation coverage at 8 km spatial resolution and 15 day temporal resolution were computed using data for the period 1982 to 2006, produced by the Global Inventory Monitoring and Mapping Studies (GIMMS) group from measurements of the advanced very high resolution radiometer (AVHRR) onboard the NOAA 7, NOAA 9, NOAA 11, and NOAA 14 satellites. Data from the National Center for Environmental Prediction/National Center for Atmospheric Research (NCEP/NCAR) Reanalysis Project (Kalnay et al., 1996) were also used in this study. The variables selected for analysis were the monthly mean geopotential height, monthly mean wind, daily mean sea level pressure and daily mean wind from 1961 to 2013 on a 2.5°×2.5° spatial grid (<http://www.esrl.noaa.gov/psd/>).

## 4 Results

### 245 4.1 Spatial characteristics of extreme precipitation

Figure 3a shows that the mean annual precipitation (for the period 1961-2015) varied from 115 mm in the northwest to the 845 mm in the southeastern LP. The associated EPTs ranged from 17 mm·d<sup>-1</sup> in northwest to 50 mm·d<sup>-1</sup> from in southeast (Figure 3b); these EPT isohyets are generally consistent with these of mean annual precipitation. Figure 3b indicates that the area around the Dongsheng station is a regional EP center since that the EPTs around the station are higher than these of the surrounding areas, whereas the isohyets of mean annual precipitation are smooth. The spatial distribution of MEPs is also similar to that of mean annual precipitation, increasing from northwest to southeast and ranging from 35 to 138 mm·yr<sup>-1</sup>, as shown in Figure 3c. Maximums of MEP occur in the southern and southeastern LP.

Figure 3d indicates that EPFs over the region during the past five decades have ranged from 54 days to 115 days (the i.e., mean annual EPF ranged from 1.0 to 2.1 d). Notable occurrences of high EPF can be seen in and around the Ziwuling Mountains in the mid-southern LP, while the highest frequency occurred at the east of the Fenhe Valley in the southeastern LP. Meanwhile, the lowest frequency occurred in the northwestern LP, the western Muus sandy land, and the western Liupan Mountains.

Figure 3e indicates that the averaged EPIs ranged mainly between 0.3 and 0.7. The spatial variations of EPI and EPF contrast with each other, with highest EPIs centered in the mid-eastern LP, where EPFs were comparatively lower, and lowest EPIs in the southeastern LP, which had the maximum mean annual precipitation and EPF. The highest values of EPI dominated the Central LP area. The northern boundary of the area was positioned southeast of the Muus Desert (Dongsheng and Xingxian and Yulin cities) and south of the Baiyu Mountains (Wuqi and Huanxian counties); the western boundary was positioned west of the Liupan Mountains (Haiyuan Guyuan, Jingyuan and Yuzhong counties); the eastern boundary was positioned northeast of the Luliang Mountains and Fenhe Valley (Taiyuan and Linfen); the southern boundary was positioned to the north of the Central Shaanxi Plain (Huashan, Xi'an and Changwu). The EPI presents the event-EP-power causing natural hazards. This high value of EPI in part explains why this area is characterized by very serious soil erosion that releases more than 2-billion ton sediment annually into channels of the Yellow River.

Figure 3f indicates that the spatial distribution of EPS in the LP increased from northwest to southeast, ranging from 0.27 to 0.66, but with the highest EPSs centered in the southeast Central LP. The areas with highest EPSs covered the basins of the Jing, Luo, and Fen rivers. Although an EP event always occurred over a small range, the spatial maps of EPI, EPF, and EPS indicate that the areas with serious EP events are regularly distributed.

### 4.3.2 Spatiotemporal variation of EP

Our results (Figure 4a) indicate that 91.4% of the LP was characterized by a negative annual precipitation trend over the study period, whereas only 8.6% of the total area presented a positive trend. There were 9 out of 87 stations showed significant

275 negative trend while 2 stations showed positive trends ( $p < 0.1$ ). At the same time, the spatiotemporal trends of the annual EP ranged from -0.78 to +0.48 mm·~~yr~~<sup>-1</sup> (Figure 4b), with 23.8% of the total area showing a positive trend, with increased annual EP distributed mainly in the southwestern LP (west of Lanzhou) and the mid-southern LP (Beiluo and Jing river basins and an area around the Xingxian station). Meanwhile, the annual EPF changed by -0.6 to +0.5 ~~days~~ over the past 55 years, with a change rate ranging from  $-1.2 \times 10^{-2}$  to  $+0.95 \times 10^{-2}$  ~~d~~<sup>ays</sup>/yr<sup>-1</sup>, as shown in Figure 4c. Of the 87 stations, 4 stations showed  
280 significant negative trend of EPF while 3 stations showed positive trends ( $p < 0.1$ ). The areas with a negatively trending EPF covered 86.4% of the total area while the areas with positively trending EPF covered 13.6%, the latter occurring mainly in the southwestern LP (around the Xining station) and in the areas around the Xi'an and Xingxian stations. The areas with notably decreasing trends occurred mainly in the mid-west and southeast regions of the LP.

Figure 4d indicates that the changes of annual EPI ranged from -0.18 to +0.27, with a change rate ranging from  $-0.34 \times$   
285  $10^{-2}$  to  $0.52 \times 10^{-2}$  ~~yr~~<sup>-1</sup>. We found that 34 of the 87 stations showed a-upward slopes (5 stations with a significance level  $p < 0.1$ ), and 53 stations (4 stations with a significance level  $p < 0.1$ ) showed a-negative slopes. As shown in Figure 4d, areas with positive trends of EPI accounted for 42.2% of the total area, with the areas delineating by the Wulate-Yulin-Yan'an-Huashan stations and the Jingtai-Xiji-Tianshui stations, as well as the area west of the Minhe station. The areas with a negative slope covered 57.8% of the total area.

290 Figure 4e indicates that the annual EPSs changed by -0.09 to +0.07 during the study period, with rates varying from  $-0.34 \times 10^{-2}$  to  $0.52 \times 10^{-2}$  yr<sup>-1</sup>. Of the 87 stations, 39 stations showed a positive slope (3 stations with a significance level of  $p < 0.05$ ), while 54 stations exhibited a negative slope (4-2 station with a significance level of  $p < 0.05$ ). The areas with increased EPSs covered 25.4% of the total area and were mainly found in an area delineated by the Wuqi, Tianshui, and Huashan stations and an area west of the Xiji station. The areas with negative trends accounted for 74.6% of the total area.

295 The trends estimates computed for annual EP, EPF, and EPI are associated with strong uncertainty. For instance, the upward trend of annual EP in and around the Xingxian station relied heavily on the upward trend of the EPF and not the downward trend of the EPI. The EPF around the Changwu station decreased, but both the annual EP and EPS increased with the upward trend of the EPI. However, nearly all the areas with positive trends for annual EP, EPI, EPF, and EPS had a negative trend in  
300 positive-EP indices with positive trends, potentially indicating the risk of more serious hazardous situations.

### 4.3 Intra-annual EP characteristics and their relationship to large-scale atmospheric circulation

#### 4.3.1 The intra-annual Distribution of EP events

Figure 5 displays the intra-annual distributions of the MDP and the ADEP for the 87 stations from 1961 to 2015. Precipitation from June to September accounts for 72% of the total amount, while 91% of the total EP events occur from June  
305 to August. According to the fitted curve (Figure 5), the highest MDP occurred on July 26, which is 11 days earlier than the

maximum ADEP on 6 August. Based on fitting the four-parameter Weibull curve ( $p < 0.0001$ ), the MDP for the 224 days from March 26 to November 4 accounted for 95% of the mean annual precipitation. Meanwhile, the ADEP from May 21 to September 18 accounted for 95% of the total EPF.

310 Therefore, high concentration of amount of daily precipitation into a limited period results in a significant alternation of wet and dry seasons in the LP. In addition, low precipitation but with annual alteration of dry and wet seasons, and highly concentrated intra-annual EP events with an occurrence 11 days earlier than the wettest days, contributes to a fragile environment subject to severe natural hazards. Specifically, lower precipitation but highest EPI and EPS are responsible for the most severe hazard situations in the Central LP, such as soil erosion.

#### 4.3.2 Atmospheric circulation factors for the spatial variation of extreme precipitation

315 Atmospheric circulation is the leading factor causing the above phenomena. The LP is located in the East Asian monsoon region. According to the average sea level pressure and winds ~~at the 1000-hPa level~~ in winter from 1961 to 2015 (see Figure 6a), the dry winter in the region is influenced by the interactions between two high pressure areas in Southwest China (the Tibet Plateau high pressure system) and North China (the Mongolia high pressure system). The prevailing East Asian winter monsoon (which has a north-northwest direction) circulates in East China and brings cold and dry airstreams. In contrast, the summer climate of the LP is affected by interactions between two high pressure systems, the Pacific high pressure and Tibet Plateau high pressure systems. Figure 6b shows that the prevailing East Asian summer monsoon (which has a south-southeast wind direction) brings warm and humid maritime airstreams that spread from the West Pacific to Central China. However, the Tibet Plateau high pressure has a notable effect on the climate of the northwestern LP, and the airstream humidity decreases gradually as the distance from the Pacific increases. The resulting effect and decreased humidity is to form a vast arid region in Northwest China, including the northwestern LP, with a prevailing wind direction of west-southwest. This explains why precipitation decreases from southeast to northwest, and precipitation is scarce in the northwest LP.

325 Nevertheless, tropical cyclones occasionally enter the central LP, accompanied by EP events. For instance, in August 1996 a Western Pacific cyclone landed in the southeastern coastal area of China and weakened gradually as it moved northwest, as shown by the 1000-hPa geopotential height and winds in Figure 6c. Plenty of rainstorms or intense rainfall events accompanied the cyclones occurred in its transit area. On 3 August 1996, the weakened cyclone reached the southeastern LP, as shown in Figure 6d. However, under the control of the Tibet Plateau high pressure, the central LP is generally the northwestern boundary to which the tropical cyclone can reach. As shown in Figure 6d, the cyclone was blocked from entering the northwestern LP, moved towards the northeast, and gradually dissipated. These phenomena illustrate why this region has limited precipitation but severe EP events.

### 5.1 Rationality of Spatial EP Characteristics

Natural hazards related to EP can be divided into two categories: (1) hazards accompanied by EP, and (2) hazards that follow the occurrence of EP. For the former, one focus is the dependence of EP and storm surges in the coastal zone. Using such dependence structures, EP and storm surge can be quantified to provide information for successful hazard management (Svensson and Jones, 2004; Zheng et al., 2013). For the latter, the LP is such that the area suffers from EP-induced natural hazards that exceed the general tolerance of the natural environment, existing ecosystems, human life and social economy. In this case, the rational characteristics of EP responsible for spatial hazards can be studied.

Here, we use the widely distributed soil erosion to verify the rationality of our results. According to the universal soil loss equation (Wischmeier, 1976), the rational characteristics of EP should correlate well with soil erosion and vegetation coverage (Figure 7). To examine this, partial correlation analyses were performed between soil erosion intensity and EPI/EPS, and with the vegetation coverage. Our results indicate that water-based erosion intensity correlates significantly with vegetation coverage (negatively, Figure 7a) and EPS (positively, Figure 3f); the related coefficients are -0.61 ( $p < 0.001$ ) and 0.53 ( $p < 0.001$ ), respectively. For the correlations between water erosion intensity and vegetation coverage, and with EPI (Figure 3e), the coefficients are -0.58 ( $p < 0.001$ ) and 0.76 ( $p < 0.001$ ), respectively. This finding demonstrates the rationality of our results. Note that, the higher correlation between EPI and soil erosion agrees with the results of plot experiments by Tang (1993), who noted that high-intensity precipitation is the primary driving force of erosion.

Zhou and Wang (1992) divided the LP into three zones of raindrop kinetic energy (<1000, 1000–1500, and 1500–2000 J·m<sup>-2</sup>·yr<sup>-1</sup>, respectively), based on observations of the raindrop kinetic energies of rainstorms during 1980s. We found that the 30 and 35 mm/d EPT contours closely overlap with the raindrop kinetic energy contours of 1000 and 1500 J·m<sup>-2</sup>·yr<sup>-1</sup>. Further, soil erosion in the LP in recent decades has been found to be approximately 5000–10 000 t·km<sup>-2</sup>·yr<sup>-1</sup> (Ludwig and Probst, 1998; Shi and Shao, 2000). Such high rates of sediment erosion are generally induced by several rainstorm events during the year, with the top 5 daily sediment yields accounting for 70%–90% of the annual total soil loss (Rustomji et al., 2008; Zhang et al., 2017). For instance, a 200-year precipitation event in Wuqi on 30 August 1994 induced a flooding event with a daily sediment concentration of 1060 kg/m<sup>3</sup>. The streamflow was 2.41/25.6 times of the mean annual streamflow from 2002 to 2011, and the sediment load was equivalent to 9.6% of the total sediment yields from 1963 to 2011 (Zhang et al., 2016). Therefore, ~~it can be inferred~~ the EPF obtained in this study, about twice ~~a every~~ year on average, is rational to explain such serious sediment erosion.

In the LP, spring drought is the limit factor for vegetation (especially herbaceous vegetation) recovery from winter every year, and grass generally germinates on an extensive scale after the first effective rainfall event (>5 mm) in spring (Cai, 2001; Tang, 1993; Tang, 2004). However, as shown in Figure 5, the highest EPF occurred 11 days earlier than the day of maximum daily precipitation in the LP (Figure 5). This means that, the days on which the LP experiences most serious EP events, tend to be days when precipitation is less. In other words, every year, the vegetation has not sufficiently recovered when ~~the most~~

frequently EP events occur in the LP. Such an intra-annual distribution of precipitation is one of the climatic reasons why there is serious soil erosion in the semiarid LP. Further, the sparse spatial nature of precipitation is insufficient for the growth of high-coverage vegetation, especially in the northwestern ~~area~~-LP (Figure 7a). However, the highest EPI provides the strongest erosion force, which contributes to the severe rates of erosion (Figure 7b) in the Central LP. These results of EP responsible for hazardous situations in both spatial and temporal are important for sustainable catchment management, ecosystem restoration, and water resources planning and management within the LP. Given that 62.1% of the total LP with negative trend of annual precipitation has one or more positive EP indices, the underlying upward trends of water erosion and sediment yield should be taken into account in catchment management efforts.

## 375 5.2 Uncertainty in EP identification

The uncertainties in identification and assessment of EP events come from two aspects: (1) the stochasticity in climate (Miao et al., 2018) and (2) the methodology (Papalexiou et al., 2013). For the former, significant spatiotemporal variations occur in EP events as a result of varying geographical and meteorological conditions (Pinya et al., 2015). Extreme precipitation events are relatively rare, poorly predictable, and often with short duration, thus resulting in uncertainty in EP event identification. In the method section, the uncertainties in EPTs determination from parametric and non-parametric methods were discussed.

Figure 8 shows the results of EPF obtained by non-parametric methods for all 87 stations over the LP during 1961-2015. Large variances among the results, calculated at different percentile levels, are shown in Figures 8a-8c. Trivially, it can be seen that the thresholds-EPTs are smaller but with larger EPFs for lower percentiles. The 3-times standard deviation method (Figure 8d) provided similar results with similar at different standard deviation levels variance among stations in comparison with universal multifractal method (Figure 8f,g). The EPTs determined by individual methods generally increase with annual precipitation increasing. As shown in Figures ~~8d,e-8e,f~~ and 3a, there is no precipitation event exceed 50 mm·d<sup>-1</sup> as mean annual precipitation is < 200 mm in the northwestern LP. A 50 mm/d threshold is probably suitable for the Southeast LP with higher mean annual precipitation, whereas a 25 mm/d threshold may be more suitable for some stations in the northwestern LP where there are no EP event exceeding 50 mm/d. Therefore, regardless of the varying geographical and meteorological conditions, the selection of these thresholds can be quite subjective and empirical. Note that, although similar variance of EPTs among stations can be obtained by individual methods, the spatial causes for hazards situations cannot be theoretically explained by such these methods in Figures 8a-8f.

Parametric methods require a predetermined threshold value, above which the data can be chosen as the EP series if the data series passed the goodness-of-fit test. As shown in Figure 9, both fixed values and percentiles were adopted to preset EPT. The selected rainfall series data were fitted to the gamma, GPA (generalized Pareto distribution), Gumbel, Pearson type III, GEV (generalized extreme value distribution), ~~exponential~~ and the GNO (Weibull-generalized normal) distributions, whose parameters were estimated with the *L*-moments method (Haddad et al., 2011) at a 0.05 significance level, using goodness-of-fit tests including K-S (Kolmogorov-Smirnov test), A-D (Anderson-Darling K-Sample test) and C-S (Pearson's Chi-squared

test) tests. As shown in Figures 9a1-9a3 and 9b1-9b3, the results of the ~~three K-S and A-D~~ tests are similar but different in in  
400 details from those of C-S test for the preset fixed value and percentile thresholds.

Further, these results for different distribution functions are quite different from each other. As shown in Figures 9a1-9a2,  
by the K-S and A-D tests, the passing rates from GEV, ~~and~~ Gumbell, GNO and pearson type III distribution functions are high  
while there is almost very low no passing rate from GPA, ~~exponential~~ and Gamma functions. In addition, the passing rates are  
different ~~or evenly opposite~~ between preset methods of percentiles and fixed values. As shown in Figure 9, the GEV and  
405 Gumbell distribution function have high passing rates for EP series obtained by preset percentiles when percentile < 99%  
(Figures 9a1-9a2), whereas the passing rate for these series obtained by fixed values decrease with increasing values are very  
low (Figures 9b1-9b2). We also found that these distribution functions are not sensitive to the percentile or fixed value changes.  
These findings indicates that the fitting accuracy can be greatly affected by the selection of the extreme value distribution  
functions, goodness-of-fit tests and methods for EPT preset. Liu et al. (2013) noted that the fitting accuracy is also affected by  
410 the size of rainfall series. So, unavoidably, applications of parametric methods also depend on personal subjectivity and  
empiricism. We have tried to explore EP using fixed values in spatiotemporal variation of precipitation analysis in the LP;  
however, we found that the results could not well explain the rainfall-induced natural hazards or agree with these plot  
experiments in spatial (Wan et al., 2014), and the same to these results obtained by fixed values (Xin et al., 2009) and  
percentiles (Li et al., 2010a; 2010b). These uncertainties may the reason why prior studies of EP over the LP tend to disagree  
415 with each other ~~(Li et al., 2010b, 2012; Xin et al., 2009).~~

As noted by Pandey et al. (1998) and Douglas and Barros (2003), these methodological uncertainties arise due to the wide  
gap between mathematical modelling and the physical understanding of precipitation processes. As previously mentioned, the  
multifractal technique can be used to describe the statistical probability and physical processes associated with observed data  
(Lovejoy and Schertzer, 2013; Tessier et al., 1996), while the scale invariance of multifractals enables the multifractal  
420 technique to also overcome the influence of the sample size (Pandey et al., 1998; Tessier et al., 1996). Further, the segmentation  
algorithm helps to overcome the problem of uncertainty. In the present study, the general correspondence and the specific  
divergences between EPT and precipitation isohyets (Figure 3) further exhibits the varying meteorological and geographical  
influences. As shown in Table 2, by fitting EP series derived by universal multifractals to the six distribution functions, the  
100% passing rate of goodness-fit test strongly supports that universal multifractal approach is advanced in identifying EP  
425 events. Overall, the universal multifractal method provides a much superior approach to addressing uncertainties and providing  
a unique set of EPTs.

## 6. Conclusions

We have proposed an approach that integrates universal multifractals with a segmentation algorithm to enable identification  
of EP events, and thereby to assess its spatiotemporal EP characteristics in the LP, using data from 87 meteorological stations

430 from 1961 to 2015. We find that the spatial distribution of the EPTs increased from 17.3 mm/d in the northwestern to 50.3  
mm/d in the southeastern LP. Similarly, the MEP increased from 35 mm to 138 mm/yr, with the maximum MEP occurred in  
the southern and southeastern LP. The EPF over the LP was within a range of 54–116 days over the last 55 years. Notable  
occurrences of EPFs mainly observed in the mid-southern and southeastern LP. An examination of atmosphere circulation  
435 EP intensity and EP severity in this area. Correlation analysis significantly supported the reasonability of the spatial estimates  
of EP characteristics that are responsible for hazardous situations over the LP. The climate factors for the most serious  
hazardous situations in the LP especially in the Central LP come from the low precipitation, the highest EPI and the highly  
ADEP concentrated 11 days earlier than the wet season.

Spatiotemporally, annual EP increased in the southwestern and mid-southern LP. The areas with a positive EPF trend  
440 occurred in the southwestern LP and the areas around the Xi'an and Xingxian stations, whilst the areas with a positive trend  
of EPI among the Wulate-Yulin-Yan'an-Huashan stations and the Jingtai-Xiji-Tianshui stations, as well as the area west of  
the Minhe station. The annual EPSs with increased slope covered an area delineated by the Wuqi, Tianshui, and Huashan  
stations and an area west of the Xiji station. Overall, the areas with upward trends of the annual EP, EPF, EPI, and EPS  
445 accounted for 23.8%, 13.6%, 42.2%, and 25.4% of the LP area, respectively. It should be noted that 62.1% of the LP area with  
negative annual precipitation experienced upward trends of one or more EP variables. It can be concluded that EP over the LP  
intensified, potentially imposing a risk of more serious hazardous situation. Sustainable countermeasures should be considered  
in the catchment management to address the underlying hazards.

In conclusion, the universal multifractal approach considers both the physical processes and their probability distribution,  
and thereby provides an approach to overcome uncertainties and identify EP events without the need for empirical adjustments.  
450 This approach is thus useful for application to spatiotemporal EP assessment at regional scale.

*Data availability.* All the data used in this study are available upon request.

*Author contributions.* JZ, XZ and RL prepared the research project. JZ, HVG, GG BF and CW conceptualised the methodology.  
JZ developed the code and performed the analysis. JZ prepared the manuscript with contributions from all co-authors.

*Competing interests.* The authors declare that they have no conflict of interest.

#### 455 **Acknowledgements:**

This research was funded by the National Natural Science Foundation of China (no. 41701207), the State Key Project of  
Research and Development Plan of China (no. 2016YFC0501603), the Open Foundation of the State Key Laboratory of Urban  
and Regional Ecology of China (no. SKLURE2019-2-5), and the Fundamental Research Funds for the Central Universities of

China (no. 2652018034). The corresponding author acknowledges partial support by the Australian Centre of Excellence for  
460 Climate System Science (CE110001028). We thank the China Meteorological Data Sharing Service System, the Yellow River  
Conservancy Commission, the LP Science Data Centre of the Data Sharing Infrastructure of Earth System Science of China,  
and the NCEP/NCAR for providing data used in this paper. All data sources are publicly accessible and these websites are  
listed in Section 3.2.

## References

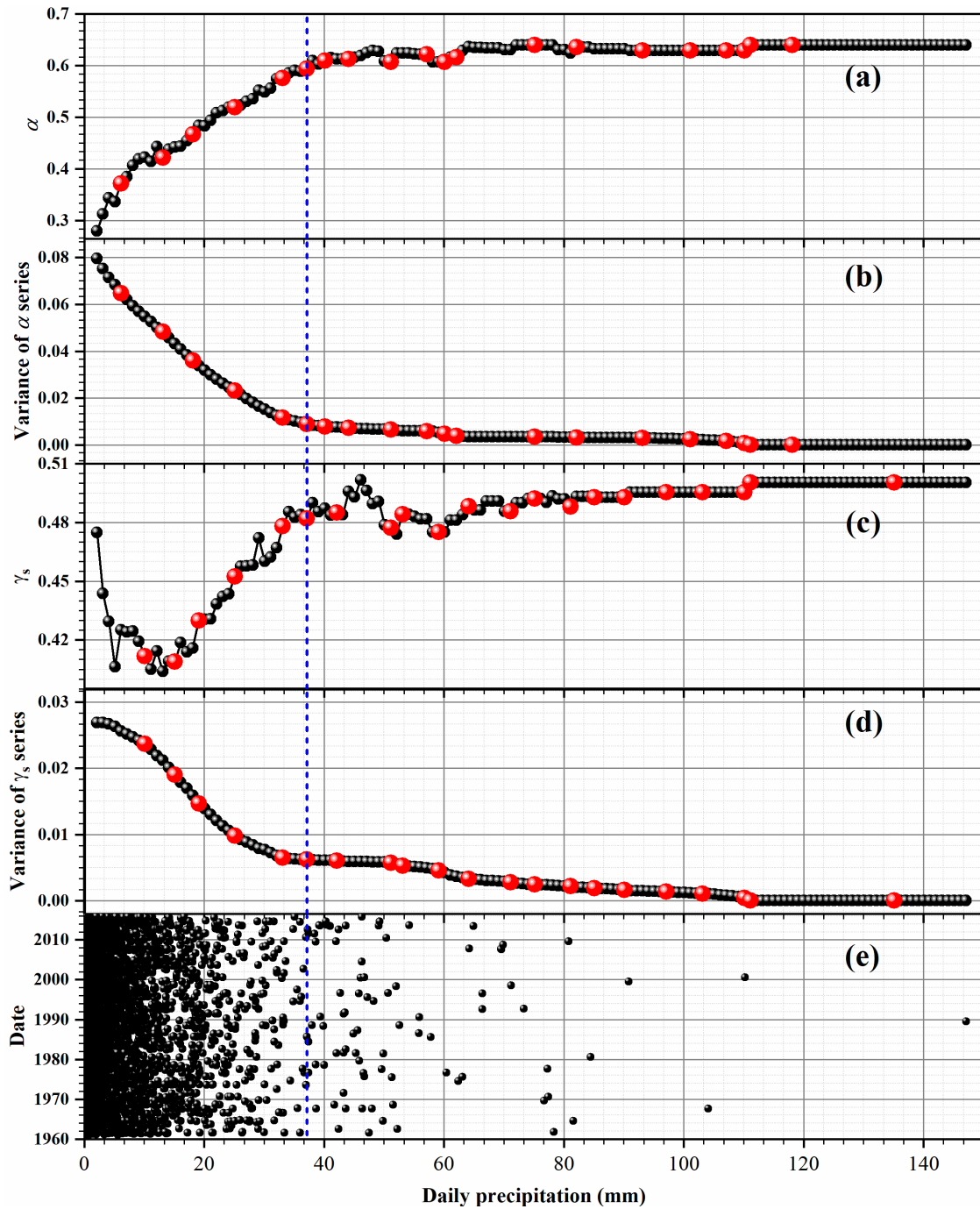
- 465 Anagnostopoulou, C. and Tolika, K.: Extreme precipitation in Europe: statistical threshold selection based on climatological  
criteria, *Theor. Appl. Climatol.*, 107, 479-489, 2012.
- Bao, J., Sherwood, S. C., Alexander, L. V., and Evans, J. P.: Future increases in extreme precipitation exceed observed scaling  
rates, *Nature Clim. Change*, 7, 128, 2017.
- Beguiría, S., Vicente - Serrano, S. M., López - Moreno, J. I., and García - Ruiz, J. M.: Annual and seasonal mapping of peak  
470 intensity, magnitude and duration of extreme precipitation events across a climatic gradient, northeast Spain, *Int. J.*  
*Climatol.*, 29, 1759-1779, 2009.
- Bernaola Galván, P., Ivanov, P. C., Amaral, L. A. N., and Stanley, H. E.: Scale invariance in the nonstationarity of human heart  
rate, *Phys. Review Lett.*, 87, 168-105, 2001.
- Cai, Q.: Soil erosion and management on the Loess Plateau, *J. Geogr. Sci.*, 11, 53-70, 2001.
- 475 Deidda, R. and Puliga, M.: Sensitivity of goodness-of-fit statistics to rainfall data rounding off, *Phys. Chem. Earth*, 31, 1240-  
1251, 2006.
- Donat, M. G., Lowry, A. L., Alexander, L. V., O’Gorman, P. A., and Maher, N.: More extreme precipitation in the world’s dry  
and wet regions, *Nature Clim. Change*, 6, 508, doi: : 10.1038/NCLIMATE2941, 2016.
- Dong, Q., Chen, X., and Chen, T.: Characteristics and Changes of Extreme Precipitation in the Yellow--Huaihe and Yangtze--  
480 Huaihe Rivers Basins, China, *J. Climate*, 24, 3781-3795, 2011.
- Douglas, E. M. and Barros, A. P.: Probable maximum precipitation estimation using multifractals: application in the Eastern  
United States, *J. Hydrometeorol.*, 4, 1012-1024, 2003.
- Du, H., Wu, Z., Zong, S., Meng, X., and Wang, L.: Assessing the characteristics of extreme precipitation over Northeast China  
using the multifractal detrended fluctuation analysis, *J. Geophys. Res. - Atmos.*, 118, doi: 10.1002/jgrd.50487, 52013,  
485 2013.
- Dulière, V., Zhang, Y., and Salathé Jr, E. P.: Extreme precipitation and temperature over the US Pacific Northwest: A  
comparison between observations, reanalysis data, and regional models, *J. Climate*, 24, 1950-1964, 2011.
- Eekhout, J. P., Hunink, J. E., Terink, W., and de Vente, J.: Why increased extreme precipitation under climate change negatively  
affects water security, *Hydrol. Earth Syst. Sc.*, 22, 5935-5946, 2018.
- 490 Feng, X., Fu, B., Piao, S., Wang, S., Ciais, P., Zeng, Z., Lü, Y., Zeng, Y., Li, Y., and Jiang, X.: Revegetation in China’s Loess  
Plateau is approaching sustainable water resource limits, *Nature Clim. Change*, 6, 1019-1022, 2016.

- Feng, X., Sun, G., Fu, B., Su, C., Liu, Y., and Lamparski, H.: Regional effects of vegetation restoration on water yield across the Loess Plateau, China, *Hydrol. Earth Syst. Sc.*, 16, 2617-2628, 2012.
- Gagnon, J.-S., Lovejoy, S., and Schertzer, D.: Multifractal earth topography, *Nonlinear Proc. Geoph.*, 13, 541-570, 2006.
- 495 Haddad, K., Rahman, A., and Green, J.: Design rainfall estimation in Australia: a case study using L moments and generalized least squares regression, *Stoch. Env. Res. Risk A.*, 25, 815-825, 2011.
- Herold, N., Behrangi, A., and Alexander, L. V.: Large uncertainties in observed daily precipitation extremes over land, *J. Geophys. Res. - Atmos.*, 122, 668-681, 2017.
- Huang, J., Yu, H., Guan, X., Wang, G., and Guo, R.: Accelerated dryland expansion under climate change, *Nature Clim. Change*, 500 6, 166, 2016.
- Hubert, P., Tessier, Y., Lovejoy, S., Schertzer, D., Schmitt, F., Ladoy, P., Carbonnel, J., Violette, S., and Desurosne, I.: Multifractals and extreme rainfall events, *Geophys. Res. Lett.*, 20, 931-934, 1993.
- Intergovernmental Panel on Climate Change (IPCC), *Climate Change 2007: Synthesis Report. Contribution of Working Groups I, II and III to the Fourth Assessment Report of the Intergovernmental Panel on Climate Change*, edited by Core Writing Team, R. K. Pachauri, and A. Reisinger, 104 pp., Geneva, Switzerland, 2007.
- 505 Kalnay, E., Kanamitsu, M., Kistler, R., Collins, W., Deaven, D., Gandin, L., Iredell, M., Saha, S., White, G., and Woollen, J.: The NCEP/NCAR 40-year reanalysis project, *B. Am. Meteorol. Soc.*, 77, 437-471, 1996.
- Lavallée, D., Lovejoy, S., Schertzer, D., and Ladoy, P.: Nonlinear variability and landscape topography: analysis and simulation. In: *Fractals in geography*, Lam, N. S.-N. and Cola, L. D. (Eds.), PTR Prentice-Hall, London, 1993.
- 510 Li, Y., Cai, W., and Campbell, E.: Statistical modeling of extreme rainfall in southwest Western Australia, *J. Climate*, 18, 852-863, 2005.
- Li, Z., Xu, X., Xu, C., Liu, M., Wang, K., and Yu, B.: Annual Runoff is Highly Linked to Precipitation Extremes in Karst Catchments of Southwest China, *J. Hydrometeorol.*, 18, 2745-2759, 2017.
- Li, Z., Zheng, F.-l., Liu, W.-z., and Flanagan, D. C.: Spatial distribution and temporal trends of extreme temperature and precipitation events on the Loess Plateau of China during 1961–2007, *Quatern. Int.*, 226, 92-100, 2010a.
- 515 Li, Z., Zheng, F., and Liu, W.: Analyzing the spatial temporal changes of extreme precipitation events in the loess plateau from 1961 to 2007, *J. Nat. Res.*, 25, 291-299, 2010b. (in Chinese with English abstract)
- Li, Z., Zheng, F., and Liu, W.: Spatiotemporal characteristics of reference evapotranspiration during 1961–2009 and its projected changes during 2011–2099 on the Loess Plateau of China, *Agr. Forest Meteorol.*, 154, 147-155, 2012.
- 520 Liu, B., Chen, J., Chen, X., Lian, Y., and Wu, L.: Uncertainty in determining extreme precipitation thresholds, *J. Hydrol.*, 503, 233-245, 2013.
- Lovejoy, S. and Schertzer, D.: Scaling and multifractal fields in the solid earth and topography, *Nonlinear Proc. Geoph.*, 14, 465-502, 2007.
- Lovejoy, S. and Schertzer, D.: *The weather and Climate: emergent laws and multifractal cascades*, Cambridge University Press, 525 2013.

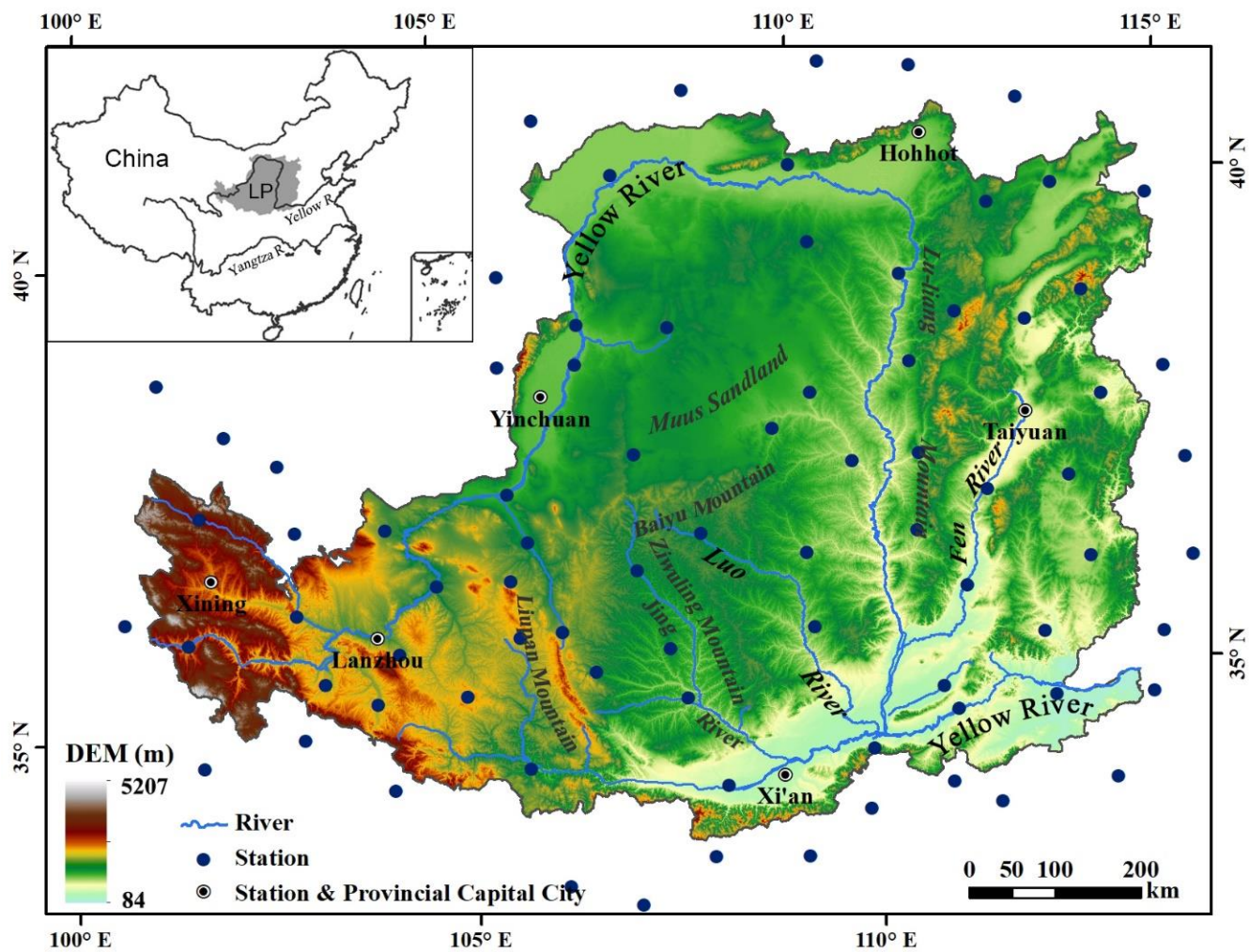
- Ludwig, W. and Probst, J. L.: River sediment discharge to the oceans; present-day controls and global budgets, *Am. J. Sci.*, 298, 265-295, 1998.
- Manola, I., Hurk, B. v. d., Moel, H. D., and Aerts, J. C.: Future extreme precipitation intensities based on a historic event, *Hydrol. Earth Syst. Sci.*, 22, 3777-3788, 2018.
- 530 Miao, C., Duan, Q., Sun, Q., Lei, X., and Li, H.: Non-uniform changes in different categories of precipitation intensity across China and the associated large-scale circulations, *Environ. Res. Lett.*, 14, doi: 10.1088/1748-9326/aaf306, 2019.
- Miao, C., Sun, Q., Duan, Q., and Wang, Y.: Joint analysis of changes in temperature and precipitation on the Loess Plateau during the period 1961–2011, *Clim. Dynam.*, 47, 3221-3234, 2016.
- Min, S., Zhang, X., Zwiers, F. W., and Hegerl, G. C.: Human contribution to more-intense precipitation extremes, *Nature*, 470, 535 378-381, 2011.
- Oliver, M. A. and Webster, R.: Kriging: a method of interpolation for geographical information systems, *Int. J. Geogr. Inf. Syst.*, 4, 313-332, 1990.
- Pandey, G., Lovejoy, S., and Schertzer, D.: Multifractal analysis of daily river flows including extremes for basins of five to two million square kilometres, one day to 75 years, *J. Hydrol.*, 208, 62-81, 1998.
- 540 Papalexiou, S., Koutsoyiannis, D., and Makropoulos, C.: How extreme is extreme? An assessment of daily rainfall distribution tails, *Hydrol. Earth Syst. Sc.*, 17, 851-862, 2013.
- Parisi, G. and Frisch, U.: A multifractal model of intermittency. In: *Turbulence and predictability in geophysical fluid dynamics and climate dynamics*, Ghil, M., Benzi, R., and G., P. (Eds.), Amsterdam, North-Holland 1985.
- Pecl, G. T., Araújo, M. B., Bell, J. D., Blanchard, J., Bonebrake, T. C., Chen, I.-C., Clark, T. D., Colwell, R. K., Danielsen, F., 545 and Evengård, B.: Biodiversity redistribution under climate change: Impacts on ecosystems and human well-being, *Science*, 355, doi: 10.1126/science.aai9214, 2017.
- Pfahl, S., O’Gorman, P. A., and Fischer, E. M.: Understanding the regional pattern of projected future changes in extreme precipitation, *Nature Clim. Change*, 7, 423, doi: 10.1038/NCLIMATE3287, 2017.
- Pinya, M. A. S., Hundecha, Y., Lawrence, D., Madsen, H., Willems, P., Martinkova, M., Vormoor, K., Bürger, G., Hanel, M., 550 and Kriauciuniene, J.: Inter-comparison of statistical downscaling methods for projection of extreme precipitation in Europe, *Hydrol. Earth Syst. Sci.*, 19, 1827-1847, 2015.
- Ran, D., Liu, L., Zhao, L., Bai, Z., Liu, B., and Wang, H.: The soil conservation practices and streamflow and sediment load changes in the Hekou-Longmen region of middle reaches of Yellow River. In: *Yellow River Water Conservancy Press, Zhengzhou* (in Chinese), 2000.
- 555 Ren, M.-e.: Sediment discharge of the Yellow River, China: past, present and future-a synthesis, *Adv. Earth Sci.*, 21, 551-563, 2006. (in Chinese with English)
- Rustomji, P., Zhang, X., Hairsine, P., Zhang, L., and Zhao, J.: River sediment load and concentration responses to changes in hydrology and catchment management in the Loess Plateau region of China, *Water Resour. Res.*, 44, W00A04, doi:10.1029/2007WR006656., 2008.

- 560 Schertzer, D. and Lovejoy, S.: Physical modeling and analysis of rain and clouds by anisotropic scaling multiplicative processes, *J. Geophys. Res. - Atmos.*, 92, 9693-9714, 1987.
- Shi, H. and Shao, M.: Soil and water loss from the Loess Plateau in China, *J. Arid Environ.*, 45, 9-20, 2000.
- Stow, D., Daeschner, S., Hope, A., Douglas, D., Petersen, A., Myneni, R., Zhou, L., and Oechel, W.: Variability of the seasonally integrated normalized difference vegetation index across the north slope of Alaska in the 1990s, *Int. J. Remote Sens.*, 24, 1111-1117, 2003.
- 565 Svensson, C. and Jones, D. A.: Dependence between sea surge, river flow and precipitation in south and west Britain, *Hydrol. Earth Syst. Sci.*, 8, 973-992, 2004.
- Swendsen, R. H. and Wang, J.-S.: Nonuniversal critical dynamics in Monte Carlo simulations, *Phys. Review Lett.*, 58, 86-88, 1987.
- 570 Tang, K.: The changes of erosion, runoff and sediment in the Yellow River, Science China Press, Beijing, 1993. (in Chinese)
- Tang, K.: Soil and water conservation in China, Science China Press, Beijing, 2004. (in Chinese)
- Tang, K.: The soil conservation practices and streamflow and sediment load changes in the Hekou-Longmen region of middle reaches of Yellow River, Yellow River Water Conservancy Press, Zhengzhou, 1990. (in Chinese)
- Tessier, Y., Lovejoy, S., Hubert, P., Schertzer, D., and Pecknold, S.: Multifractal analysis and modeling of rainfall and river flows and scaling, causal transfer functions, *J. Geophys. Res.*, 101, 26427-26426,26440, 1996.
- 575 Tessier, Y., Lovejoy, S., and Schertzer, D.: Multifractal analysis and simulation of the global meteorological network, *J. Appl. Meteorol.*, 33, 1572-1586, 1994.
- Tessier, Y., Lovejoy, S., and Schertzer, D.: Universal multifractals: theory and observations for rain and clouds, *J. Appl. Meteorol.*, 32, 223-250, 1993.
- 580 Walther, G.-R., Post, E., Convey, P., Menzel, A., Parmesan, C., Beebee, T. J., Fromentin, J.-M., Hoegh-Guldberg, O., and Bairlein, F.: Ecological responses to recent climate change, *Nature*, 416, 389, 2002.
- Wan, L., Zhang, X., Ma, Q., Zhang, J., Ma, T., and Sun, Y.: Spatiotemporal characteristics of precipitation and extreme events on the Loess Plateau of China between 1957 and 2009, *Hydrol. Process.*, 28, 4971-4983, 2014.
- Wang, G., Wang, D., Trenberth, K. E., Erfanian, A., Yu, M., Bosilovich, M. G., and Parr, D. T.: The peak structure and future changes of the relationships between extreme precipitation and temperature, *Nature Clim. Change*, 7, 268, 2017.
- 585 Wang, S., Fu, B., Piao, S., Lü, Y., Ciais, P., Feng, X., and Wang, Y.: Reduced sediment transport in the Yellow River due to anthropogenic changes, *Nature Geosci.*, 9, 38-41, 2015.
- Wischmeier, W. H.: Use and misuse of the universal soil loss equation, *J. Soil Water conserv.*, 31, 5-9, 1976.
- Xin, Z., Xu, J., and Ma, Y.: Spatio-temporal Variation of Erosive Precipitation in Loess Plateau during Past 50 Years, *Sci. Geogr. Sin.*, 29, 98-104, 2009.
- 590 Zhang, J., Zhang, T., Lei, Y., Zhang, X., and Li, R.: Streamflow regime variations following ecological management on the Loess Plateau, China, *Forests*, 7, 1-18, doi:10.3390/f7010006, 2016.

- Zhang, J., Zhang, X., Li, R., Chen, L., and Lin, P.: Did streamflow or suspended sediment concentration changes reduce sediment load in the middle reaches of the Yellow River?, *J. Hydrol.*, 546, 357-369, 2017.
- 595 Zhang, X., Walling, D. E., Quine, T. A., and Wen, A.: Use of reservoir deposits and caesium-137 measurements to investigate the erosional response of a small drainage basin in the rolling loess plateau region of China, *Land Degrad. Dev.*, 8, 1-16, 1997.
- Zheng, F., Westra, S., and Leonard, M.: Opposing local precipitation extremes, *Nature Clim. Change*, 5, 389-390, 2015.
- Zheng, F., Westra, S., and Sisson, S. A.: Quantifying the dependence between extreme rainfall and storm surge in the coastal  
600 zone, *J. Hydrology*, 505, 172-187, 2013.
- Zhou, P. and Wang, Z.: A Study on Rainstorm Causing Soil Erosion in the Loess Plateau, *J. Soil Water Conserv.*, 6, 1-5, 1992.  
(in Chinese with English abstract)



605 **Fig. 1:** Procedure for the EPT determination of the Xingxian station. (a) The multifractal index  $\alpha$  (black dots) and the alternative abrupt points (red dots). (b) Pooled variances (black dots) as calculated from the  $\alpha$  series with the significant abrupt points (red dots) of the variances. (c) As in (a) but for the singularity  $\gamma_s$ . (d) As in (b) but for the variance calculated from the  $\gamma_s$  series. (e) The time variation of daily precipitation ranging from 1961 to 2015. The blue dot line represents the determined EPT.



610 Fig. 2: Location of the Loess Plateau in the middle reaches of the Yellow River, China (inset) and distribution of the meteorological stations in and around the LP.

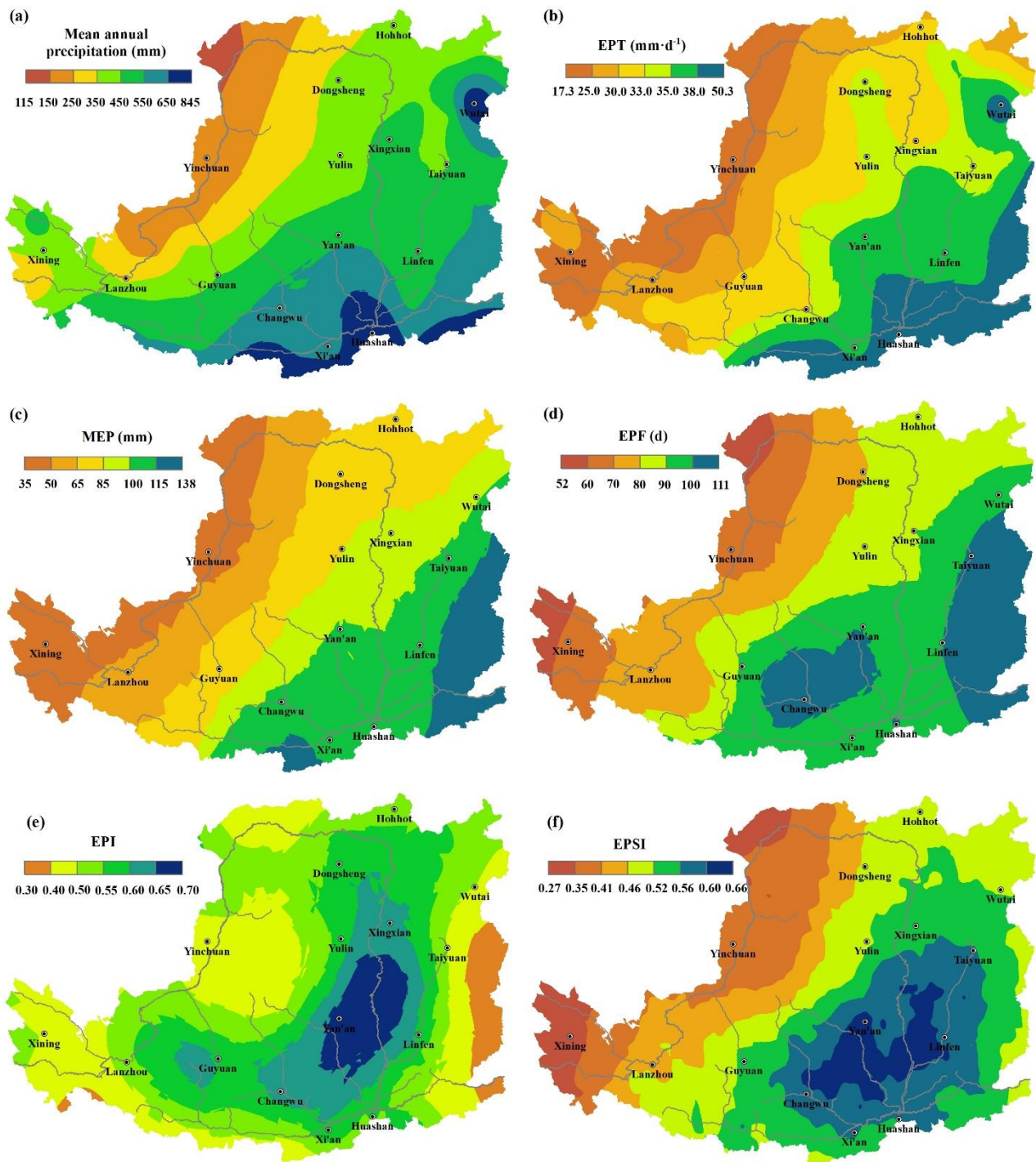
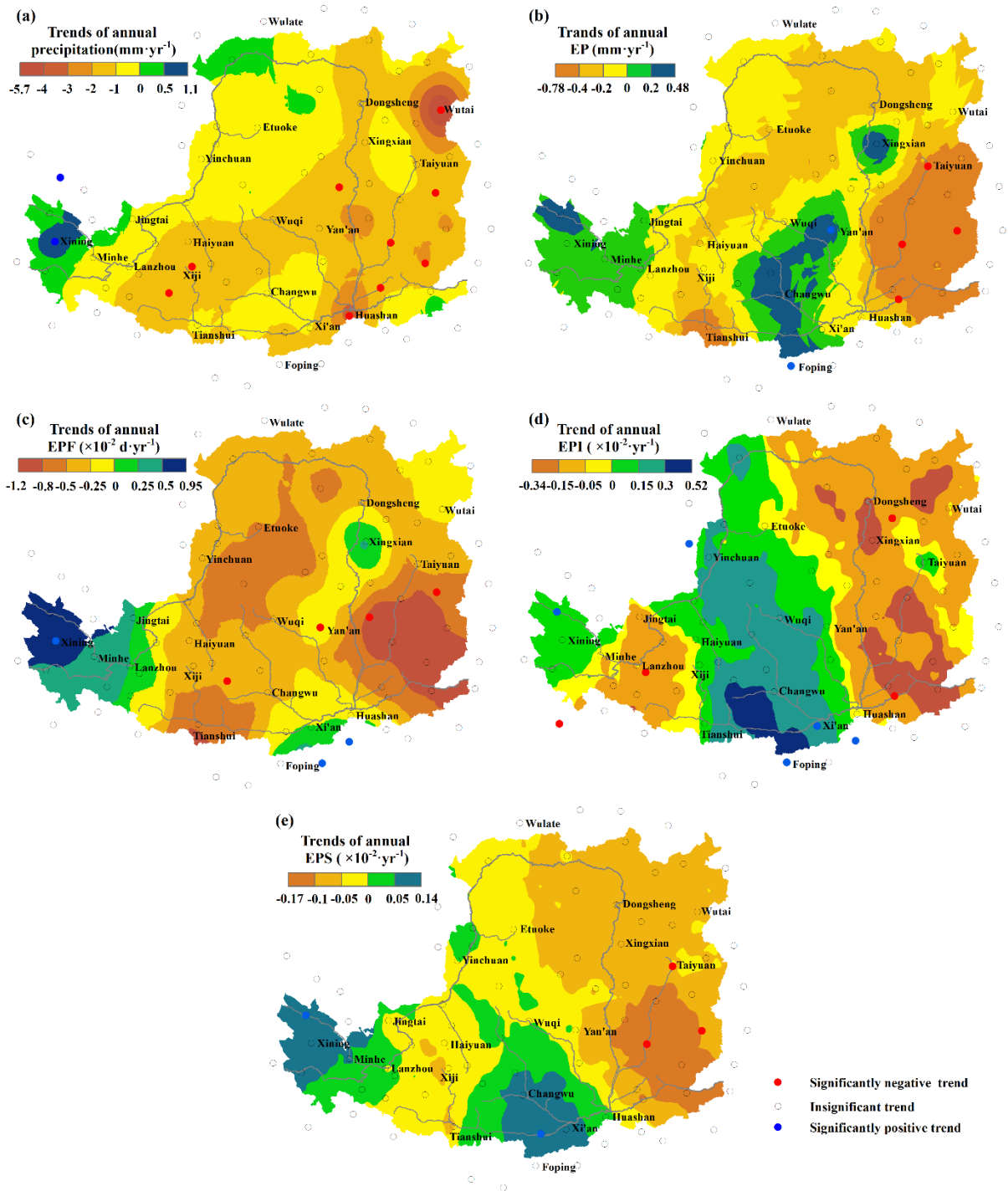


Fig. 3: Spatial distributions of (a) mean annual precipitation, (b) EPTs, (c) MEP, (d) total EPF, (e) mean EPI, and (f) mean annual EPSI in the LP from 1961 to 2015.



615 Fig. 4: The spatial distribution of the trends **and the stations with significant trend ( $p < 0.1$ )** for (a) annual precipitation, (b) annual EP, (c) annual EPF, (d) annual EPI, and (e) annual EPS in the LP from 1961 to 2015.

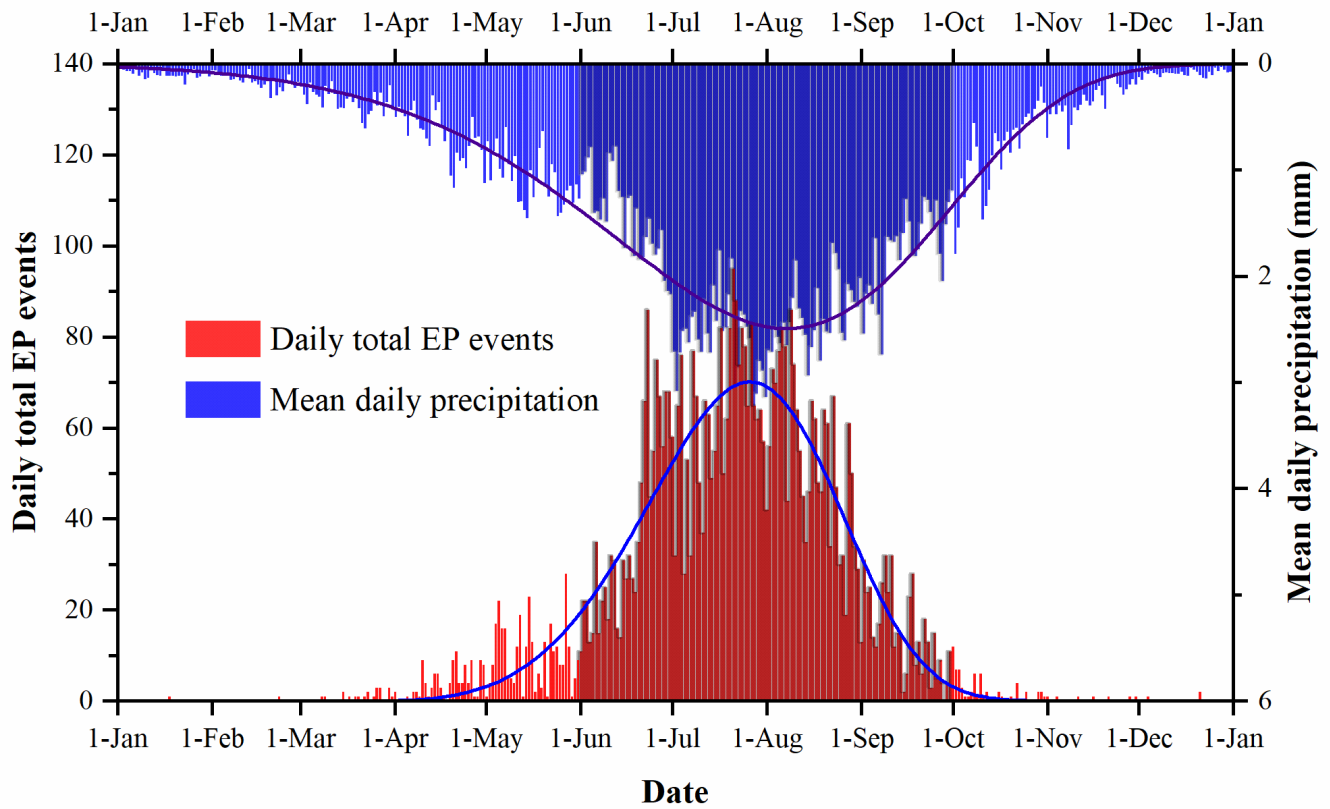
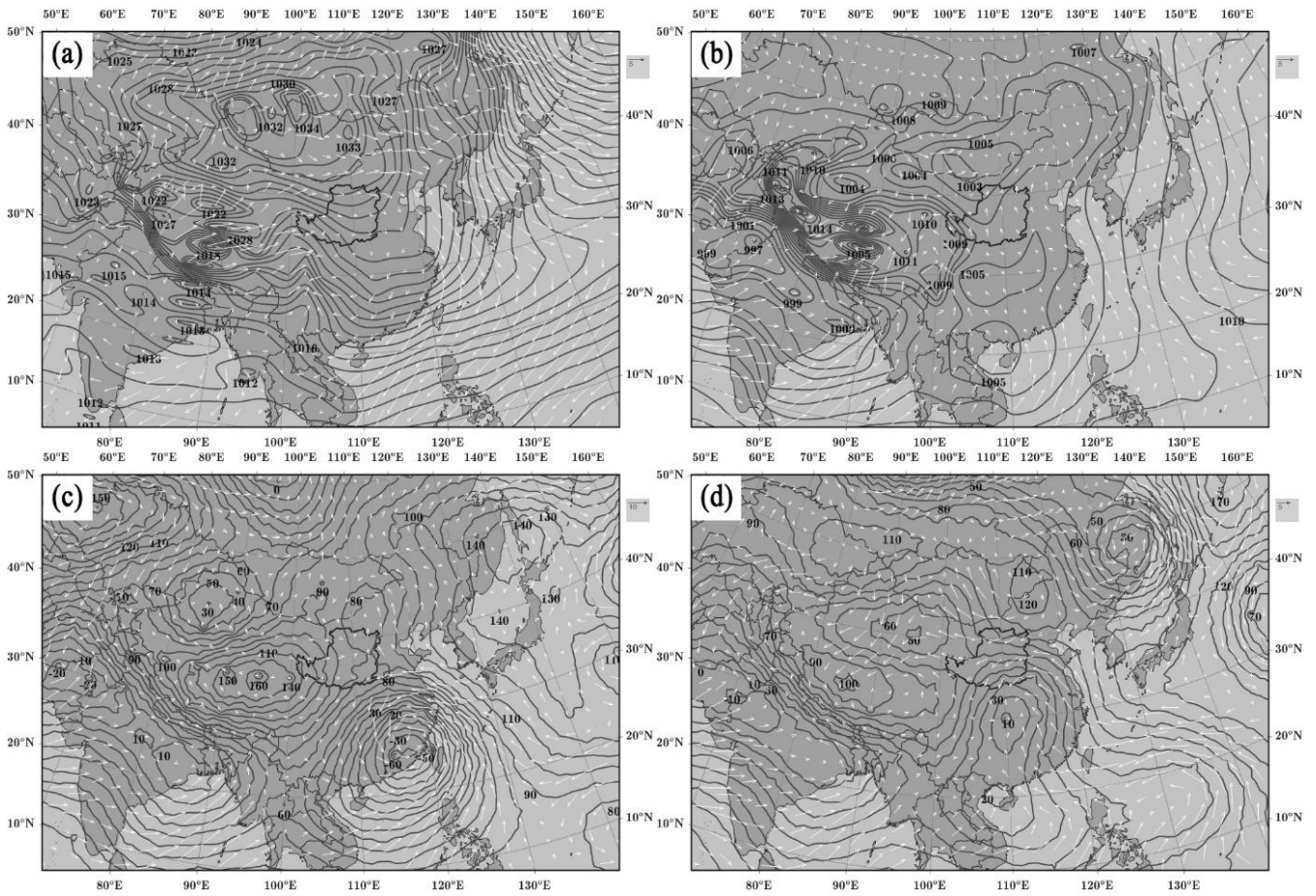
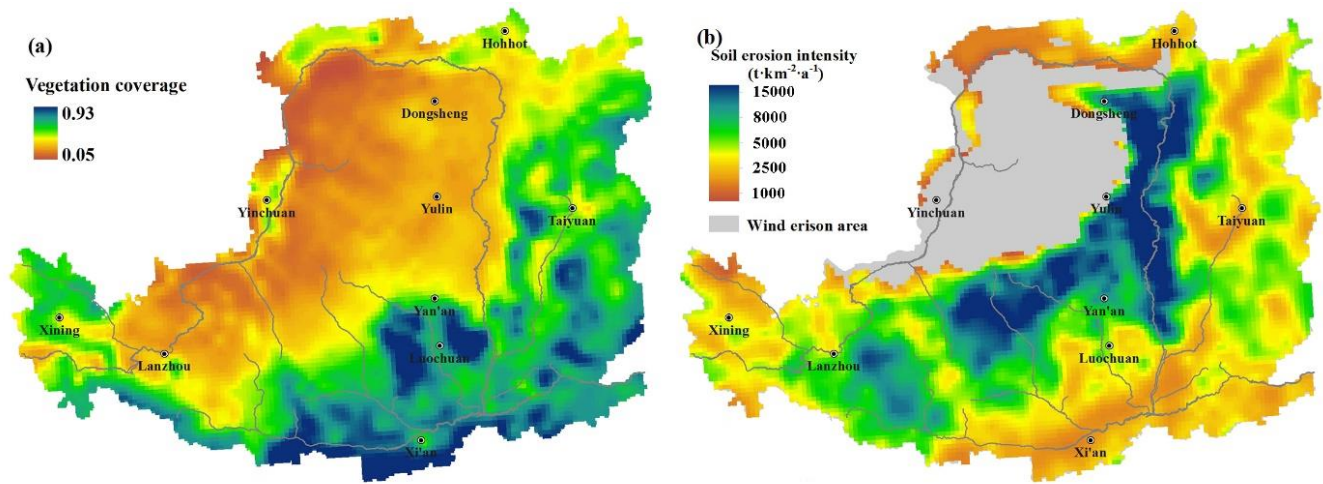


Fig. 5: Intra-annual distribution of daily precipitation (MDP) and the number of daily EP events (ADEP) for the 87 stations from 1961 to 2015 and their fitting curves by Weibull function.



620

**Figure 6: Average sea level pressure and winds: (a) the mean for all winters (from December to February) and (b) the mean for all summers (from June to August) from 1961 to 2015; Characteristics of average 1000-hPa geopotential height and winds on (c) 1 August 1996 and (d) 3 August 1996. The data were derived from global NCEP/NCAR reanalysis average monthly and daily data.**



625 Fig. 7: (a) Spatial distribution of mean vegetation coverage in summer (from June to August) on the Loess Plateau from 1982 to 2006 at a spatial resolution of 8 km. (b) Spatial distribution of the soil erosion intensity, which was resampled to a spatial resolution 8 km.

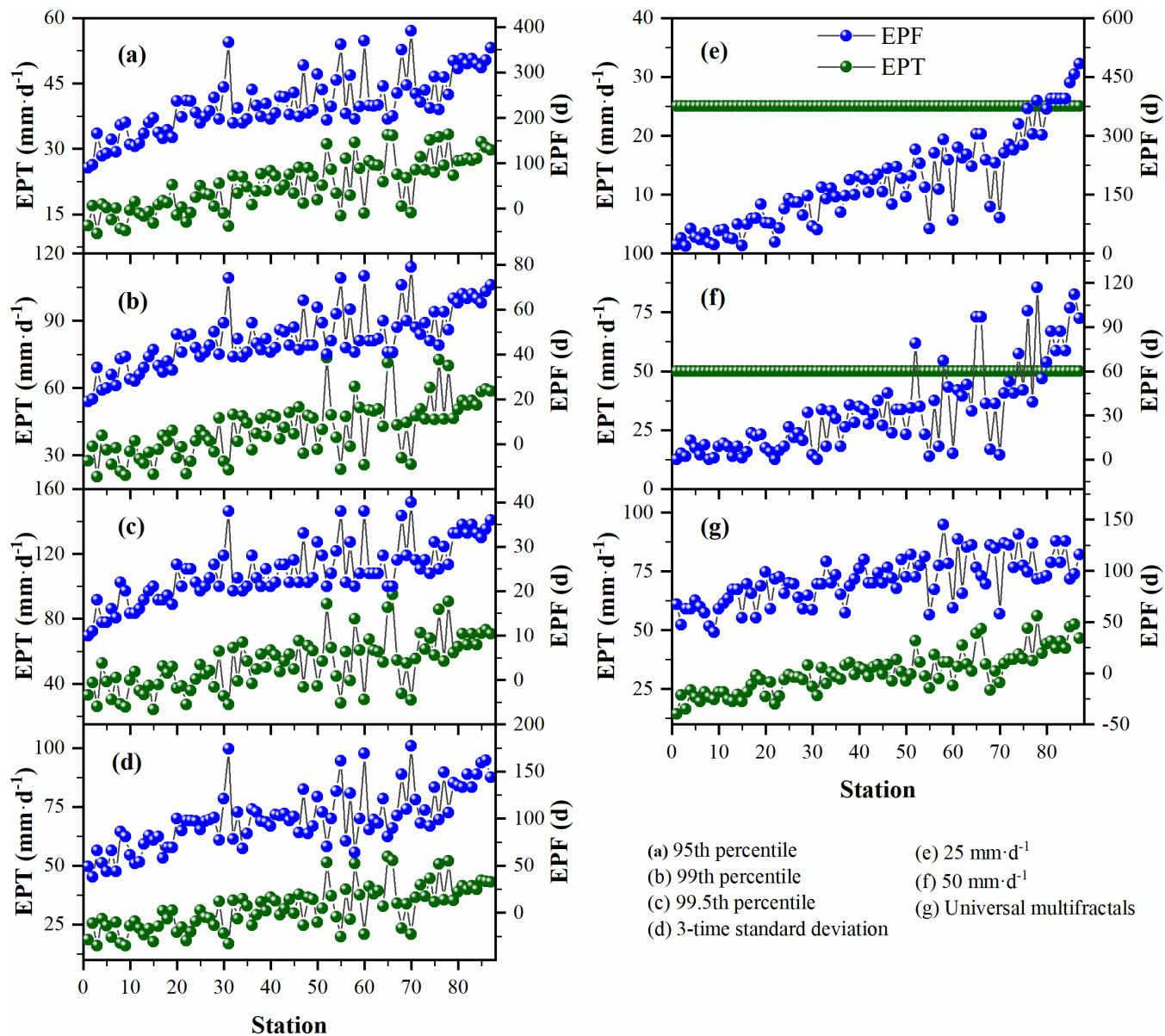


Fig. 8: EPTs determined by different methods and the corresponding EP frequencies for 87 stations over the Loess Plateau. The abscissa represents the stations with an increase in mean annual precipitation from 104 mm to 918 mm. The signs in Figures 8a–8e display EPT and EPF derived by the 95th, 99th and 99.5th percentiles, respectively, while the signs in Figures 8d–8f display the EPF and the fixed thresholds 25 mm/d, 50 mm/d and the EPT derived by the three-time standard deviation method, respectively.

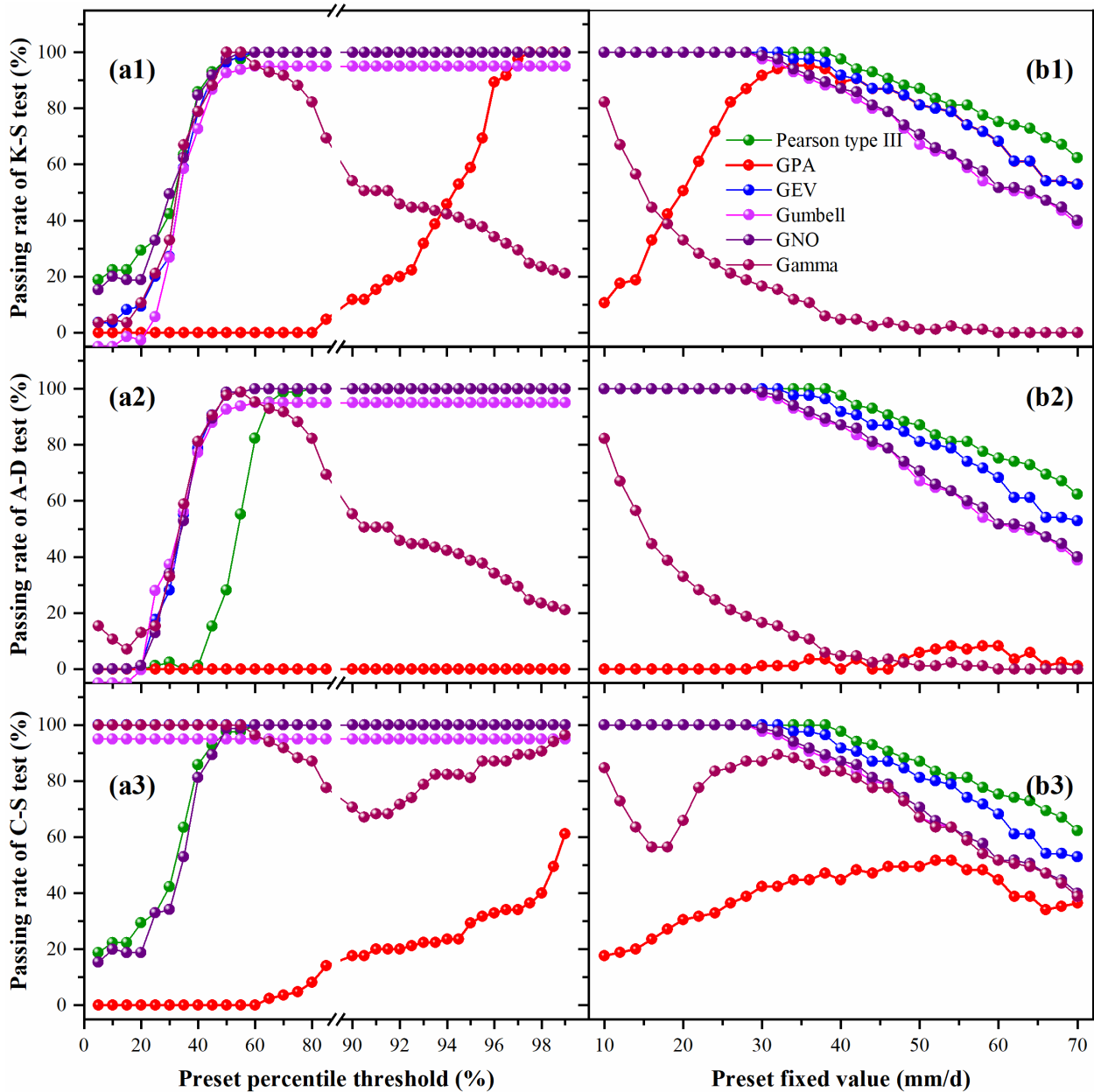


Figure 9: The passing rates of goodness-of-fit test for individual distribution functions, with EP data series selected by different preset thresholds. (a1) K-S test, (a2) A-D test and (a3) C-S test for different distribution functions using preset percentile thresholds. (b1) K-S test, (b2) A-D test and (b3) C-S test for different distribution functions using thresholds of fixed values. The significant level is 0.05. The symbol lines of the passing rate of Gumbell Gumbell-functions in a1-a3 and those of the Exponential function in a1-a2 and b1-b3 in figures a1, a2 and a3 were offset upward arbitrarily offset by -5 upward arbitrarily by 5 units, respectively and the passing rate of Weibull function in a1-a2 were offset upward arbitrarily by 10 units to separate them.

635

**Table 1: Indices (abbreviations) used in this study addressing precipitation variations.**

<u>Index</u> <u>Abbreviation</u>	<u>Definition</u> <u>Variables</u>	Units
EPT	extreme precipitation threshold	mm <del>/d</del> <sup>d<sup>-1</sup></sup>
MEP	mean annual extreme precipitation	mm
EPF	frequency of extreme precipitation event	d
EPI	intensity of extreme precipitation event	dimensionless
EPSI	severity of extreme precipitation event	dimensionless
MDP	long-term mean intra-annual daily precipitation	mm <del>/d</del>
ADEP	long-term accumulated intra-annual daily extreme precipitation events	d

640

Table 2. Passing rates of goodness-of- fit test for EP events determined by universal multifractals method.

<u>Function</u>	<u>K-S test (%)</u>	<u>A-D test (%)</u>	<u>C-S test (%)</u>
<u>Gamma</u>	<u>100</u>	<u>100</u>	<u>100</u>
<u>GPA</u>	<u>100</u>	<u>100</u>	<u>100</u>
<u>Gumbell</u>	<u>100</u>	<u>100</u>	<u>100</u>
<u>Pearson type III</u>	<u>100</u>	<u>100</u>	<u>100</u>
<u>GEV</u>	<u>100</u>	<u>100</u>	<u>100</u>
<u>GNO</u>	<u>100</u>	<u>100</u>	<u>100</u>